Structural and Multidisciplinary Optimization (2022) 65:21
https://doi.org/10.1007/s00158-021-03123-7

RESEARCH PAPER

Reliability-based design optimization under dependent random variables by a generalized polynomial chaos expansion

Dongjin Lee[1] · **Sharif Rahman**[1]

Received: 6 July 2021 / Revised: 15 September 2021 / Accepted: 12 October 2021 / Published online: 27 December 2021

Abstract
This article brings forward a new computational method for reliability-based design optimization (RBDO) of complex mechanical systems subject to input random variables following arbitrary, dependent probability distributions. It involves a generalized polynomial chaos expansion (GPCE) for reliability analysis subject to dependent input random variables, a novel fusion of the GPCE approximation and score functions for estimating the sensitivities of the failure probability with respect to design variables, and standard gradient-based optimization algorithms, resulting in a multi-point single-step design process. The method, designated as the multi-point single-step GPCE method or simply the MPSS-GPCE method, yields analytical formulae for computing the failure probability and its design sensitivities concurrently from a single stochastic simulation or analysis. For this reason, the MPSS-GPCE method affords the ability to solve industrial-scale problems with large design spaces. Numerical results stemming from mathematical functions or elementary engineering problems indicate that the new method provides more accurate or computationally efficient design solutions than existing methods or reference solutions. Furthermore, the shape design optimization of a jet engine compressor blade root was successfully conducted, demonstrating the power of the new method in confronting practical RBDO problems.

Keywords RBDO · Reliability analysis · GPCE · Design sensitivity analysis · Score functions · Stochastic optimization

1 Introduction

Reliability-based design optimization (RBDO) is an important paradigm for engineering design when confronted with uncertainties stemming from manufacturing processes and operating environments. (Agarwal and Renaud 2006; Chiralaksanakul and Mahadevan 2004; Du and Chen 2004; Kuschel and Rackwitz 1997; Liang et al. 2007; Rahman and Wei 2008; Ren et al. 2016; Tu et al. 1999). Typically performed in conjunction with probabilistic descriptions of the objective and/or constraint functions, RBDO of mechanical systems aims to achieve high reliability of an optimal design by satisfying the constraints at desired probability levels. On the other hand, robust design optimization (RDO)—another major archetype for design under uncertainty—strives to improve the product quality by minimizing the objective function considering the mean and variance of a performance function, leading to an insensitive design. The objective function of RDO can also be integrated with the probabilistic constraints of RBDO, which is regarded as an extension of RBDO or reliability-based robust design optimization. New studies concerning RBDO, the focus of this work, are being reported almost every year with real-world applications, such as those found in the design of aerospace (Hassan and Crossley 2008; Nannapaneni and Mahadevan 2020), automotive (Youn et al. 2004; Gu et al. 2015), civil (Siavashi and Eamon 2019), and electronic structures (Kang et al. 2017) or devices (Li et al. 2019).

Existing RBDO algorithms in the past were heavily dominated by the first-order reliability method (FORM), which involves estimating the failure probability by a linear approximation of the performance function at the most probable point (MPP) (Du and Chen 2004; Kuschel and Rackwitz 1997; Tu et al. 1999). Depending on how FORM is incorporated into the optimization process, the RBDO algorithms can be grouped into three main classes: double-loop algorithms (Tu et al. 1999); single-loop algorithms (Kuschel and

Responsible Editor: Byeng D. Youn

✉ Dongjin Lee
dongjin-lee@uiowa.edu

[1] Department of Mechanical Engineering, The University of Iowa, Iowa City, IA 52242, USA

Rackwitz 1997); and decoupled algorithms (Du and Chen 2004). A conventional double-loop RBDO requires nested design and reliability iteration loops and can be performed in conjunction with either the reliability index or the performance measure approaches (Tu et al. 1999). Nonetheless, it is expensive, because for each design (outer) iteration, a set of reliability (inner) iterations involving costly function evaluations must be generated for locating MPP. To reduce the high computational cost, single-loop formulations exploiting the Karush–Kuhn–Tucker optimality condition at MPP have emerged (Kuschel and Rackwitz 1997). In addition, several researchers have reformulated the nested RBDO problem to decouple reliability analysis from design optimization (Du and Chen 2004). However, a fundamental ingredient of all three classes of RBDO algorithms is FORM, which may not provide accurate reliability estimates in high dimensions and for highly nonlinear functions. Indeed, Rahman and Wei (Rahman and Wei 2008) reported that an RBDO solution using FORM and its second-order cousin, the second-order reliability method (SORM), may produce infeasible or inaccurate designs. While the subsequent developments of univariate decomposition (Rahman and Wei 2008) and dimension reduction (Lee et al. 2008) methods provide better approximations than FORM/SORM, they are still predicated on MPP. As a result, the two latter methods also become problematic or ineffective if the MPP cannot be found, as in a noisy function, or if there are multiple MPPs, as in an oscillatory function.

Numerous other studies on RBDO have been reported using multiple surrogate approximations, including polynomial response surface (Youn and Choi 2004), polynomial chaos expansion (Suryawanshi and Ghosh 2016), polynomial dimensional decomposition (Ren et al. 2016), support vector machine (Yang and Hsieh 2013), artificial neural network (Lehkỳ et al. 2018), and Kriging (Zhao et al. 2011). However, the foregoing methods, as well as many others not listed here for brevity, are largely predicated on the assumption that input variables follow independent probability distributions. Usually, in reality, there exists significant correlation or dependence among input variables (Noh et al. 2009; Lee and Rahman 2020). Indeed, neglecting these correlations or dependencies, whether emanating from loads, material properties, or manufacturing variables, may produce inaccurate or unknowingly risky designs. Only a few studies, such as those rooted in copula-based approaches (Noh et al. 2009; Lee et al. 2011), have been reported for tackling dependent random variables. Although such copula or other available variants are practical to implement, finding the right copula, when the joint distribution of random variables is arbitrary but unknown, is often not obvious. The authors here rule out the Rosenblatt transformation (Rosenblatt 1952) or others, commonly used for mapping dependent to independent variables, since they themselves may produce overly large nonlinearity to a random response, potentially degrading the convergence behavior of probabilistic solutions (Rahman 2009a). Therefore, the existing methods must be generalized or new methods should be developed from the beginning for uncertainty quantification (UQ) or reliability analysis to cope with dependent input random variables.

In a prior work, the authors developed a practical version of the generalized polynomial chaos expansion (GPCE) for UQ analysis under arbitrary, dependent input random variables (Lee and Rahman 2020). A distinguishing feature of this work, in contrast to the prequel (Rahman 2018), is that the multivariate orthonormal polynomial basis functions consistent with any non-product-type probability measure of input random variables can be numerically obtained without the need for a Rodrigues-type formula. Moreover, the GPCE approximation has been successfully employed for statistical moment and its design sensitivity analyses, leading to a computationally efficient solution of an RDO problem under dependent input random variables (Lee and Rahman 2021). However, it remains challenging to adopt the GPCE for solving RBDO problems, addressing the following questions: (1) how to simultaneously determine design sensitivity of reliability for a given design without added computational cost, (2) how to sidestep repetitive calculations of reliability and its design sensitivities to the extent possible during design iterations, and (3) how to markedly reduce the number of function evaluations or finite element analysis (FEA) in conjunction with standard gradient-based optimization algorithms for problems with large design spaces. Only by addressing these challenging issues successfully will the GPCE method have tangible advantages for solving RBDO problems subject to dependent random variables.

This paper presents a new computational method for RBDO of complex mechanical systems in the presence of input random variables endowed with arbitrary, dependent probability distributions. The method is based on (1) a GPCE for reliability analysis subject to dependent input random variables; (2) a novel fusion of the GPCE approximation and score functions for estimating the sensitivities of the failure probability with respect to design variables; and (3) standard gradient-based optimization algorithms, resulting in a multi-point single-step design process. The paper is organized as follows. Section 2 defines a general RBDO problem with the concomitant mathematical statements. Section 3 briefly presents GPCE for reliability analysis, exploiting a three-step algorithm to construct a measure-consistent multivariate orthonormal polynomial basis and standard least squares to estimate the expansion coefficient. Section 4 presents the explicit form of the score function and discloses the new analytical sensitivity method by embedding score functions with GPCE. Section 5 illustrates the multi-point single-step design process for solving RBDO and explains how the GPCE-based methods for

reliability and design sensitivity analyses are coupled with a gradient-based optimization algorithm. Section 6 involves four numerical examples, ranging from simple mathematical functions to an industrial-scale engineering problem, conducted to determine the accuracy, convergence properties, and computational efforts of the proposed method. In Sect. 7, the novelty of this work and future works are discussed. Finally, Sect. 8 presents the conclusions of this work.

2 Reliability-based design optimization

Let $\mathbb{N}$, $\mathbb{N}_0$, $\mathbb{R}$, and $\mathbb{R}_0^+$ be the sets of positive integer, non-negative integer, real number, and non-negative real number, respectively. For a positive integer $N \in \mathbb{N}$, denote by $\mathbb{R}^N$ the N-dimensional real vector space. Finally, denote by $\mathbb{A}^N \subseteq \mathbb{R}^N$ and $\bar{\mathbb{A}}^N \subseteq \mathbb{R}^N$ two bounded or unbounded domains.

Consider a measurable space $(\Omega_{\mathbf{d}}, \mathcal{F}_{\mathbf{d}})$, where $\Omega_{\mathbf{d}}$ is a sample space and $\mathcal{F}_{\mathbf{d}}$ is a σ-field on $\Omega_{\mathbf{d}}$. Defined over $(\Omega_{\mathbf{d}}, \mathcal{F}_{\mathbf{d}})$, let $\{\mathbb{P}_{\mathbf{d}} : \mathcal{F}_{\mathbf{d}} \to [0,1]\}$ be a family of probability measures where, for $M \in \mathbb{N}$ and $N \in \mathbb{N}$, $\mathbf{d} = (d_1, \cdots, d_M)^T \in \mathcal{D}$ is an M-dimensional design vector with non-empty closed set $\mathcal{D} \subset \mathbb{R}^M$. Here, $\mathbf{X} := (X_1, \cdots, X_N)^T : (\Omega_{\mathbf{d}}, \mathcal{F}_{\mathbf{d}}) \to (\mathbb{A}^N, \mathcal{B}^N)$ is an $\mathbb{A}^N$-valued input random vector with $\mathcal{B}^N$ representing the Borel σ-field on $\mathbb{A}^N$, describing the statistical uncertainties in loads, material properties, and geometry of a complex mechanical system. The probability law of $\mathbf{X}$ is completely defined by a family of the joint probability density functions (PDF) $\left\{f_{\mathbf{X}}(\mathbf{x};\mathbf{d}) : \mathbf{x} \in \mathbb{R}^N, \mathbf{d} \in \mathcal{D}\right\}$ that are associated with probability measures $\{\mathbb{P}_{\mathbf{d}} : \mathbf{d} \in \mathcal{D}\}$, so that the probability triple $(\Omega_{\mathbf{d}}, \mathcal{F}_{\mathbf{d}}, \mathbb{P}_{\mathbf{d}})$ of $\mathbf{X}$ depends on $\mathbf{d}$. In theory, a design variable d_k can be any distribution parameter or a statistic; however, here, d_k is limited to the mean of random variable X_k. Indeed, the design parameters as mean values are commonly used in almost all engineering problems.

Let $y_l(\mathbf{X}) := y_l(X_1, \ldots, X_N)$, $l = 0, 1, \ldots, K$, represent a collection of $(K+1)$ real-valued, square-integrable, measurable transformations on $(\Omega_{\mathbf{d}}, \mathcal{F}_{\mathbf{d}})$, describing performance functions of a complex system. It is assumed that $y_l : (\mathbb{A}^N, \mathcal{B}^N) \to (\mathbb{R}, \mathcal{B})$ is not an explicit function of $\mathbf{d}$, although y_l implicitly depends on $\mathbf{d}$ via the probability law of $\mathbf{X}$. This is not a major limitation, as most, if not all, RBDO problems involve means of random variables as design variables. Also, let $\mathcal{D} = \times_{k=1}^{M} [d_{k,L}, d_{k,R}]$ be a closed rectangular subregion of $\mathbb{R}^M$.

Two mathematical formulations of RBDO—one narrated with respect to the original input random variables and the other stated with respect to transformed input random variables—are discussed in the rest of this section. The formulations are equivalent because they lead to matching solutions to a general design optimization problem. However, the latter is more advantageous than the former in light of GPCE approximations, as will be further explained in upcoming sections.

2.1 Original formulation

The mathematical formulation for RBDO, defined in terms of an objective function $c_0 : \mathcal{D} \to \mathbb{R}$ and constraint functions $c_l : \mathcal{D} \to \mathbb{R}$, where $l = 1, \ldots, K$ and $1 \le K < \infty$, demands one to (Ren et al. 2016; Tu et al. 1999)

$$\begin{aligned} &\min_{\mathbf{d} \in \mathcal{D} \subseteq \mathbb{R}^M} c_0(\mathbf{d}), \\ &\text{subject to } c_l(\mathbf{d}) := \mathbb{P}_{\mathbf{d}}[\mathbf{X} \in \Omega_{F,l}(\mathbf{d})] - p_l \le 0, \\ &l = 1, \ldots, K, \\ &d_{k,L} \le d_k \le d_{k,U},\ k = 1, \ldots, M. \end{aligned} \tag{1}$$

Here, $\Omega_{F,l}(\mathbf{d})$ is the lth failure domain, $0 \le p_l \le 1$ is the lth target failure probability, and $d_{k,L}$ and $d_{k,U}$ are the lower and upper bounds of the kth design variable d_k. The objective function c_0 is commonly prescribed as a deterministic function of $\mathbf{d}$, describing relevant system geometry, such as area, volume, and mass. In contrast, the constraint functions c_l, $l = 1, 2, \ldots, K$, are generally more complicated than the objective function. Depending on the failure domain $\Omega_{F,l}$, a component or a system failure probability can be envisioned. For component reliability analysis, the failure domain is often adequately described by a single performance function $y_l(\mathbf{X})$, for instance, $\Omega_{F,l} := \left\{\mathbf{x} : y_l(\mathbf{x}) < 0\right\}$, whereas multiple, interdependent performance functions $y_{l,i}(\mathbf{x})$, $i = 1, 2, \ldots$, are required for system reliability analysis, leading, for example, to $\Omega_{F,l} := \{\mathbf{x} : \cup_i y_{l,i}(\mathbf{x}) < 0\}$ and $\Omega_{F,l} := \left\{\mathbf{x} : \cap_i y_{l,i}(\mathbf{x}) < 0\right\}$ for series and parallel systems, respectively. In any case, the evaluation of the failure probability in (1) is fundamentally equivalent to calculating a high-dimensional integral over a complex failure domain.

The evaluation of probabilistic constraints $c_l(\mathbf{d})$, $l = 1, 2, \cdots, K$, requires calculating component- or system-based probabilities of failure defined by respective performance functions. A coupling with gradient-based optimization algorithms demands that the gradients of $c_l(\mathbf{d})$ also be formulated, thus expecting design sensitivity analysis of failure probability. The essence of this work is to solve a general RBDO problem described by (1) for arbitrary functions $y_l(\mathbf{X})$, $l = 1, 2, \ldots, K$, and arbitrary, non-product-type probability distributions of $\mathbf{X}$.

2.2 Alternative formulation

Since the design variables are considered as the statistical means of some or all input random variables, a linear transformation, such as the shifting or scaling of random variables, yields an alternative formulation of RBDO. To

do so, let $(X_{i_1},\dots,X_{i_M})^\intercal$ be an M-dimensional subvector of $\mathbf{X} := (X_1,\dots,X_N)^\intercal, 1 \le i_1 \le \cdots \le i_M \le N, M \le N$, such that the mean of its kth component is the kth design variable, as follows: $\mathbb{E}_{\mathbf{d}}[X_{i_k}] = d_k, k = 1,\dots,M$.

Shifting Let $\mathbf{Z} := (Z_1,\dots,Z_N)^\intercal$ be an N-dimensional vector of new random variables obtained by shifting $\mathbf{X}$ as

$$\mathbf{Z} = \mathbf{X} + \mathbf{r}, \tag{2}$$

where $\mathbf{r} := (r_1,\dots,r_N)^\intercal$ is an N-dimensional vector of deterministic variables. Define $g_i := \mathbb{E}_{\mathbf{d}}[Z_i]$ as the mean of the ith component of $\mathbf{Z}$. Denote by $(Z_{i_1},\dots,Z_{i_M})^\intercal$ a subvector of $\mathbf{Z}$, where the i_kth new random variable Z_{i_k} corresponds to the i_kth original random variable X_{i_k}. Then, the mean of Z_{i_k} from the shifting transformation is

$$\mathbb{E}_{\mathbf{d}}[Z_{i_k}] = d_k + r_{i_k} = g_k$$

and the PDF of $\mathbf{Z}$ is

$$f_{\mathbf{Z}}(\mathbf{z};\mathbf{g}) = |\mathbf{J}| f_{\mathbf{X}}(\mathbf{x};\mathbf{d}) = f_{\mathbf{X}}(\mathbf{x};\mathbf{d}) = f_{\mathbf{X}}(\mathbf{z}-\mathbf{r};\mathbf{d}),$$

supported on the domain of $\mathbf{Z}$, say, $\bar{\mathbb{A}}^N \subseteq \mathbb{R}^N$. Here, the absolute value of the determinant of the Jacobian matrix is $|\mathbf{J}| = |\det[\partial\mathbf{x}/\partial\mathbf{z}]| = 1$ and the M-dimensional vector $\mathbf{g} := (g_1,\dots,g_M)^\intercal$ has its kth component such that $g_k = \mathbb{E}_{\mathbf{d}}[Z_{i_k}], k = 1,\dots,M$.

Scaling Let $\mathbf{Z} := (Z_1,\dots,Z_N)^\intercal$ be an N-dimensional vector of new random variables obtained by scaling $\mathbf{X}$ as

$$\mathbf{Z} = \mathrm{diag}[r_1,\dots,r_N]\mathbf{X}, \tag{3}$$

where $\mathbf{r} := (r_1,\dots,r_N)^\intercal$ is an N-dimensional vector of deterministic variables. Define $g_i := \mathbb{E}_{\mathbf{d}}[Z_i]$ as the mean of the ith component of $\mathbf{Z}$. Denote by $(Z_{i_1},\dots,Z_{i_M})^\intercal$ a subvector of $\mathbf{Z}$, where the i_kth new random variable Z_{i_k} corresponds to the i_kth original random variable X_{i_k}. Then, the mean of Z_{i_k} from the scaling transformation is

$$\mathbb{E}_{\mathbf{d}}[Z_{i_k}] = d_k r_{i_k} = g_k$$

and the PDF of $\mathbf{Z}$ is

$$\begin{aligned} f_{\mathbf{Z}}(\mathbf{z};\mathbf{g}) =& |\mathbf{J}| f_{\mathbf{X}}(\mathbf{x};\mathbf{d}) = \left|\frac{1}{r_1\dots r_N}\right| f_{\mathbf{X}}(\mathbf{x};\mathbf{d}) \\ =& \left|\frac{1}{r_1\dots r_N}\right| f_{\mathbf{X}}(\mathrm{diag}[1/r_1,\dots,1/r_N]\mathbf{z};\mathbf{d}), \end{aligned}$$

supported on the domain of $\mathbf{Z}$, say, $\bar{\mathbb{A}}^N \subseteq \mathbb{R}^N$. Here, the absolute value of the determinant of the Jacobian matrix is $|\mathbf{J}| = |\det[\partial\mathbf{x}/\partial\mathbf{z}]| = \left|1/(r_1\dots r_N)\right|$ and the M-dimensional vector $\mathbf{g} := (g_1,\dots,g_M)^\intercal$ has its kth component such that $g_k = \mathbb{E}_{\mathbf{d}}[Z_{i_k}], k = 1,\dots,M$.

For each $l = 1,2,\dots,K$, define $h_l(\mathbf{Z};\mathbf{r}) := y_l(\mathbf{X})$ to be the generic output function of the new random variables $\mathbf{Z}$, where the relation between $\mathbf{Z}$ and $\mathbf{X}$ is obtained by either the shifting transformation in (2) or the scaling transformation in (3). In both cases, the RBDO formulation requires one to

$$\begin{aligned} &\min_{\mathbf{d}\in\mathcal{D}\subseteq\mathbb{R}^M} c_0(\mathbf{d}), \\ &\text{subject to } c_l(\mathbf{d}) := \mathbb{P}_{\mathbf{g}(\mathbf{d})}[\mathbf{Z} \in \bar{\Omega}_{F,l}(\mathbf{d})] - p_l \le 0, \\ &l = 1,\dots,K, \\ &d_{k,L} \le d_k \le d_{k,U},\ k = 1,\dots,M, \end{aligned} \tag{4}$$

where $\bar{\Omega}_{F,l}(\mathbf{d})$ is the lth failure domain such that $\bar{\Omega}_{F,l} := \{\mathbf{z} : h_l(\mathbf{z};\mathbf{r}) < 0\}$ for component reliability analysis of a performance function $h_l(\mathbf{z};\mathbf{r})$, and $\bar{\Omega}_{F,l} := \{\mathbf{z} : \cup_i h_{l,i}(\mathbf{z};\mathbf{r}) < 0\}$ or $\{\mathbf{z} : \cap_i h_{l,i}(\mathbf{z};\mathbf{r}) < 0\}$ if at least two performance functions $h_{l,i}(\mathbf{z};\mathbf{r})$, $i = 1,2,\dots$, are involved in series or parallel systems, respectively, for system reliability analysis.

The alternative formulation in (4) is a restatement of (1) with respect to the new transformed input random variables $\mathbf{Z}$. In this formulation, the probability measure of $\mathbf{Z}$ is fixed during design iterations, thus sidestepping the need to recompute measure-associated quantities. For the remainder of the paper, the solution of an RBDO problem will be reported with respect to the alternative formulation. Furthermore, $\mathbf{X}$ or $\mathbf{Z}$ and y_l or h_l will be referred to, interchangeably, as input random vector and output function, respectively.

2.3 Construction of subproblems

A gradient-based solution to the RBDO problem in (4) dictates adequate smoothness in objective and constraint functions. Therefore, both functions are assumed to be differentiable with respect to design variables. Moreover, as these functions are usually nonlinear, iterative approximations of (4), leading to a sequence of RBDO subproblems, are necessary.

Let $q = 1,2,\dots,Q, Q \in \mathbb{N}$, be the design iteration count indicating the qth RBDO subproblem for (4). Given q, denote by $\mathbf{d}^{\{q\}}$, $\mathbf{g}^{\{q\}}$, and $\mathbf{r}^{\{q\}}$ the qth iterative versions of $\mathbf{d}$, $\mathbf{g}$, and $\mathbf{r}$, respectively. Then the qth RBDO subproblem demands one to

$$\begin{aligned} &\min_{\mathbf{d}^{\{q\}}\in\mathcal{D}\subseteq\mathbb{R}^M} c_0^{\{q\}}(\mathbf{d}^{\{q\}}) := T\left[c_0(\mathbf{d}^{\{q\}})\right] \\ &\text{subject to } c_l^{\{q\}}(\mathbf{d}^{\{q\}}) := T\left[\mathbb{P}_{\mathbf{g}^{\{q\}}}[\mathbf{Z} \in \bar{\Omega}_{F,l}(\mathbf{d}^{\{q\}})] - p_l\right] \le 0, \\ &l = 1,\dots,K, \\ &d_{k,L} \le d_k^{\{q\}} \le d_{k,U},\ k = 1,\dots,M, \end{aligned} \tag{5}$$

where $c_0^{\{q\}}$ and $c_l^{\{q\}}$ are, respectively, the objective and the constraint functions in the qth RBDO subproblem. They are usually obtained from first- or higher-order Taylor series expansions T of c_0 and c_l at qth initial design $\mathbf{d}_0^{\{q\}} = (d_{1,0}^{\{q\}},\dots,d_{M,0}^{\{q\}})^\intercal$. The optimal solution of (5), denoted

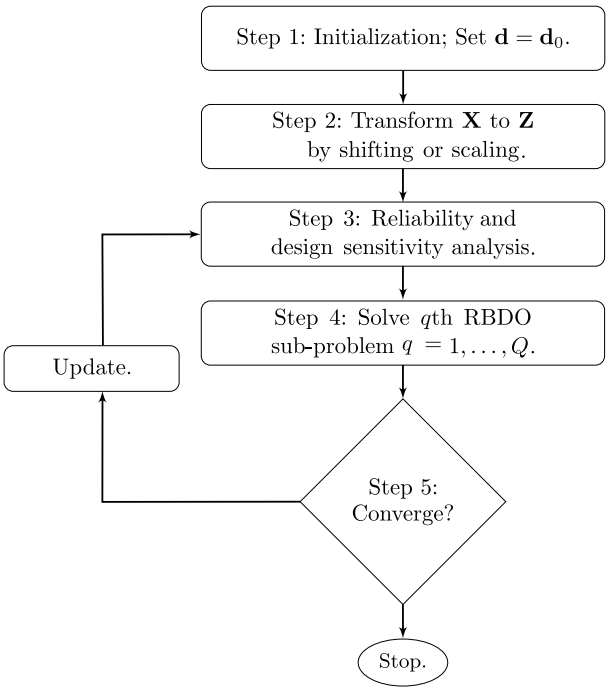

Fig. 1 A schematic description of RBDO process by a sequence of subproblems to get the final optimum $\mathbf{d}^*$

by $\mathbf{d}_*^{\{q\}} = (d_{1,*}^{\{q\}}, \ldots, d_{M,*}^{\{q\}})^\intercal$, can be produced using a suitable programming method, such as the sequential linear or quadratic programming methods. Subsequently, the qth RBDO subproblem solution $\mathbf{d}_*^{\{q\}}$ is set as the initial design $\mathbf{d}_0^{\{q+1\}}$ for the $(q+1)$th RBDO subproblem. This process is iterated from a chosen initial design $\mathbf{d}_0 = \mathbf{d}_0^{\{1\}}$ to the final optimal design $\mathbf{d}^* = \mathbf{d}_*^{\{Q\}}$ during $Q \in \mathbb{N}$ iterations to reach convergence. In this paper, the count q indicates the qth design iteration.

Overall, the original RBDO problem in (1) is solved by the following steps. The flow chart is described in Fig. 1.

1. Choose an initial design vector $\mathbf{d}_0$ and set $\mathbf{d} = \mathbf{d}_0$. Define a tolerance $0 < \epsilon < 1$.
2. Transform the input random vector $\mathbf{X}$ to a new random vector $\mathbf{Z}$ such that $\mathbb{E}_{\mathbf{d}}[Z_{i_k}] = g_k = 0$ or $1, k = 1, \ldots, M$, by shifting or scaling, respectively, described in Sect. 2.2.
3. At the current design vector $\mathbf{d}$, implement reliability analysis to estimate the failure probabilities of performance functions $h_l, l = 1, \ldots, K$, in (4). Perform design sensitivity analysis for the failure probabilities. The detail of this step will be introduced in Sects. 3 and 4.
4. Set $\mathbf{d}_0^{\{q\}} = \mathbf{d}$. Solve qth RBDO subproblem in (5) iteratively from $q = 1$ to $q = Q$ to obtain the converged optimum $\mathbf{d}_*^{\{Q\}}$.
5. If $||\mathbf{d} - \mathbf{d}_*^{\{Q\}}|| < \epsilon$, stop the process. Then the final RBDO solution is $\mathbf{d}^* = \mathbf{d}_*^{\{Q\}}$. Otherwise, update $\mathbf{d} = \mathbf{d}_*^{\{Q\}}$ and go to Step 3.

3 Reliability analysis

Given an input random vector $\mathbf{Z} := (Z_1, \ldots, Z_N)^\intercal$ with known PDF $f_{\mathbf{Z}}(\mathbf{z};\mathbf{g})$, let $h(\mathbf{Z};\mathbf{r})$ represent any one of the random output functions $h_l(\mathbf{Z};\mathbf{r}), l = 1, \ldots, K$, presented in Sect. 2. Then, the reliability analysis, required for evaluating the probabilistic constraints in (4), involves the calculation of the failure probability

$$\begin{aligned} \mathbb{P}_{\mathbf{g}}\left[\mathbf{Z} \in \bar{\Omega}_F\right] &:= \int_{\bar{\mathbb{A}}^N} I_{\bar{\Omega}_F}(\mathbf{z};\mathbf{r}) f_{\mathbf{Z}}(\mathbf{z};\mathbf{g}) d\mathbf{z} \\ &:= \mathbb{E}_{\mathbf{g}}\left[I_{\bar{\Omega}_F}(\mathbf{Z};\mathbf{r})\right], \end{aligned} \tag{6}$$

where $\bar{\Omega}_F$ is the failure domain and $I_{\bar{\Omega}_F}$ is an indicator function, such that

$$I_{\bar{\Omega}_F} = \begin{cases} 1, & \mathbf{z} \in \bar{\Omega}_F, \\ 0, & \mathbf{z} \notin \bar{\Omega}_F. \end{cases}$$

Depending on the failure domain, as explained in Sect. 2, $\bar{\Omega}_F := \{\mathbf{z} : h(\mathbf{z};\mathbf{r}) < 0\}$ for component reliability analysis and $\bar{\Omega}_F := \{\mathbf{z} : \cup_i h_i(\mathbf{z};\mathbf{r}) < 0\}$ or $\{\mathbf{z} : \cap_i h_i(\mathbf{z};\mathbf{r}) < 0\}$ for series or parallel system reliability analyses, respectively. The following subsections describe the GPCE approximation of $h(\mathbf{Z};\mathbf{r})$, formerly introduced by the authors Lee and Rahman (2020), which has been combined with an embedded Monte Carlo simulation (MCS) for reliability analysis under arbitrary, dependent input random variables.

3.1 Measure-consistent multivariate orthonormal polynomials

When $\mathbf{Z} = (Z_1, \ldots, Z_N)^\intercal$ consists of statistically dependent random variables, the joint probability measure, in general, is not a product-type. In other words, the joint probability distribution of $\mathbf{Z}$ cannot be strictly expressed by the product of its marginal probability distributions. As a result, measure-consistent multivariate orthonormal polynomials of $\mathbf{z} = (z_1, \ldots, z_N)^\intercal$ cannot be produced from N-dimensional tensor products of measure-consistent univariate orthonormal polynomials. In this section, a three-step algorithm, rooted in a whitening transformation of the monic polynomial basis, is introduced to create multivariate orthonormal polynomials consistent with an arbitrary, non-product-type probability measure $f_{\mathbf{Z}}(\mathbf{z};\mathbf{g})d\mathbf{z}$ of $\mathbf{Z}$. Note that this is a modified version of the three-step algorithm introduced by Lee and Rahman (2020), where the monomial basis is now being replaced with the monic polynomial basis to alleviate the inherent ill-conditioned problems stemming from the monomial basis. Further detail of this modified version will be presented in the latter part of this section. However, readers who are interested in more background information about

the original three-step algorithm should review the prior work (Lee and Rahman 2020).

3.1.1 Monic orthogonal polynomials

Let $f_{Z_i}(z_i)$ be the marginal PDF of the random variable Z_i under the probability measure $dF_{Z_i}(z_i) = f_{Z_i}(z_i)dz_i$, which has finite moments of an arbitrary order. For any pair of functions $u_i(z_i)$ and $v_i(z_i)$, define an inner product

$$\big(u_i(z_i), v_i(z_i)\big)_{dF_{Z_i}} := \int_{\bar{\mathbb{A}}} u_i(z_i)v_i(z_i)f_{Z_i}(z_i)dz_i$$

with respect to the probability measure $dF_{Z_i}(z_i)$. Then, monic real polynomials $\pi_{i,j_i} = z_i^{j_i} + \ldots$, $j_i = 0, 1, 2, \ldots$, are called monic orthogonal polynomials with respect to the measure $dF_{Z_i}(z_i)$ if

$$\big(\pi_{i,j_i}(z_i), \pi_{i,k_i}(z_i)\big)_{dF_{Z_i}} = 0$$

for $j_i \neq k_i$, $j_i, k_i = 0, 1, 2, \ldots$. There are infinitely many monic orthogonal polynomials if the index set $\{j_i = 0, 1, 2, \ldots\}$ is unbounded and finitely many otherwise.

The monic orthogonal polynomials $\pi_{i,j_i}(z_i)$, $j_i = 0, 1, 2, \ldots$ can be determined from the well-known three-term recurrence relation (Gautschi 2004; Rahman 2009a):

$$\pi_{i,j_i+1}(z_i) = (z_i - a_{i,j_i})\pi_{i,j_i}(z_i) - b_{i,j_i}\pi_{i,j_i-1}(z_i),$$
$$\pi_{i,-1}(z_i) = 0,\ \pi_{i,0}(z_i) = 1,$$

where

$$a_{i,j_i} = \frac{(z_i\pi_{i,j_i}(z_i), \pi_{i,j_i}(z_i))_{dF_{Z_i}}}{(\pi_{i,j_i}(z_i), \pi_{i,j_i}(z_i))_{dF_{Z_i}}},$$

and

$$b_{i,j_i} = \begin{cases} (\pi_{i,0}(z_i), \pi_{i,0}(z_i))_{dF_{Z_i}}, & j_i = 0, \\ \dfrac{(\pi_{i,j_i}(z_i), \pi_{i,j_i}(z_i))_{dF_{Z_i}}}{(\pi_{i,j_i-1}(z_i), \pi_{i,j_i-1}(z_i))_{dF_{Z_i}}}, & j_i = 1, 2, \ldots, \end{cases}$$

are the recursion coefficients uniquely determined by the measure $dF_{Z_i}(z_i)$. These coefficients can be obtained exactly for select continuous measures (Fernandes and Atchley 2006; Gautschi 2004). Otherwise, approximation methods, such as the Stieltjes procedure Stieltjes (1884), are still available to estimate them. In this study, the Stieltjes procedure was used, comprising three steps (Rahman 2009a): (1) approximate the given measure dF_{Z_i} by a discrete M-point measure $dF_{Z_i,M}$ such that $(1, 1)_{dF_{Z_i,M}} = 1$; (2) compute the recursion coefficients $a_{i,j_i,M} := a_{i,j_i}(dF_{Z_i,M})$ and $b_{i,j_i,M} := b_{i,j_i}(dF_{Z_i,M})$ of the discrete measure $dF_{Z_i,M}$; and (3) increase M and iterate calculations of the discrete versions of the recursion coefficients until a desired accuracy is achieved.

3.1.2 A modified three-step algorithm

Let $\mathbf{j} := (j_1, \ldots, j_N) \in \mathbb{N}_0^N$ be an N-dimensional multi-index. For $\mathbf{z} = (z_1, \ldots, z_N)^\intercal \in \bar{\mathbb{A}}^N \subseteq \mathbb{R}^N$, a multivariate monic polynomial in the real variables $z_1, \ldots, z_N$ is the product

$$\prod_{i=1}^{N} \pi_{i,j_i}(z_i) = \pi_{i,j_1}(z_1)\cdots\pi_{i,j_N}(z_N)$$

and has a total degree $|\mathbf{j}| = j_1 + \cdots + j_N$. Consider for each $m \in \mathbb{N}_0$ the elements of the multi-index set $\{\mathbf{j} \in \mathbb{N}_0^N : |\mathbf{j}| \le m\}$, which is arranged as $\mathbf{j}^{(1)}, \ldots, \mathbf{j}^{(L_{N,m})}$, $\mathbf{j}^{(1)} = \mathbf{0}$, according to a monomial order of choice. The set has cardinality

$$L_{N,m} := \sum_{l=0}^{m} \binom{N+l-1}{l} = \binom{N+m}{m}.$$

Denote by

$$\boldsymbol{\Psi}_m(\mathbf{z};\mathbf{g}) = (\Psi_1(\mathbf{z};\mathbf{g}), \ldots, \Psi_{L_{N,m}}(\mathbf{z};\mathbf{g}))^\intercal$$

an $L_{N,m}$-dimensional vector of multivariate orthonormal polynomials that is consistent with the probability measure $f_{\mathbf{Z}}(\mathbf{z};\mathbf{g})d\mathbf{z}$ of $\mathbf{Z}$. It is determined as follows.

(1) Given $m \in \mathbb{N}_0$, generate an $L_{N,m}$-dimensional column vector

$$\mathbf{P}_m(\mathbf{z}) = \left(\prod_{\substack{i=1 \\ \mathbf{j}=\mathbf{j}^{(1)}}}^{N} \pi_{i,j_i}(z_i), \prod_{\substack{i=1 \\ \mathbf{j}=\mathbf{j}^{(2)}}}^{N} \pi_{i,j_i}(z_i), \ldots, \prod_{\substack{i=1 \\ \mathbf{j}=\mathbf{j}^{(L_{N,m})}}}^{N} \pi_{i,j_i}(z_i) \right)^\intercal,$$

where $\prod_{\substack{i=1 \\ \mathbf{j}=\mathbf{j}^{(1)}}}^{N} \pi_{i,j_i}(z_i)$, of multivariate polynomials whose elements are the products of monic polynomials for $|\mathbf{j}| \le m$ arranged in the aforementioned order. It is referred to as the multivariate monic polynomial vector in $\mathbf{z} = (z_1, \ldots, z_N)^\intercal$ of degree at most m.

(2) Construct an $L_{N,m} \times L_{N,m}$ monic moment matrix of $\mathbf{P}_m(\mathbf{Z})$, defined as

$$\mathbf{G}_m := \mathbb{E}_{\mathbf{g}}\big[\mathbf{P}_m(\mathbf{Z})\mathbf{P}_m(\mathbf{Z})^\intercal\big] := \int_{\bar{\mathbb{A}}^N} \mathbf{P}_m(\mathbf{z})\mathbf{P}_m^\intercal(\mathbf{z})f_{\mathbf{Z}}(\mathbf{z};\mathbf{g})d\mathbf{z}.$$

For an arbitrary PDF $f_{\mathbf{Z}}(\mathbf{z};\mathbf{g})$, $\mathbf{G}_m$ cannot be determined exactly, but it can be estimated with satisfactory

accuracy either by numerical integration or sampling methods (Lee and Rahman 2020).

(3) Select the $L_{N,m} \times L_{N,m}$ whitening matrix $\mathbf{W}_m$ from the Cholesky decomposition of the monic moment matrix $\mathbf{G}_m$ such that

$$\mathbf{W}_m^{\intercal}\mathbf{W}_m = \mathbf{G}_m^{-1} \text{ or } \mathbf{W}_m^{-1}\mathbf{W}_m^{-\intercal} = \mathbf{G}_m.$$

Then, apply the whitening transformation to generate multivariate orthonormal polynomials from

$$\boldsymbol{\Psi}_m(\mathbf{z};\mathbf{g}) = \mathbf{W}_m\mathbf{P}_m(\mathbf{z}).$$

The success of the three-step algorithm depends on the construction of a well-conditioned monic moment matrix $\mathbf{G}_m$ for facilitating Cholesky factorization by standard techniques of linear algebra. During the original development of this algorithm (Lee and Rahman 2020), the authors encountered ill-conditioned moment matrices for large m if they are constructed using the monomial basis vector. In contrast, the monic moment matrix, because it is formed using tensor products of univariate monic orthogonal polynomials, should be close to a diagonal matrix for any arbitrary m if the correlations among input random variables are not overly large. It is expected that the condition number of $\mathbf{G}_m$ obtained employing monic polynomials should be much lower than that produced using monomials. Therefore, the improved three-step algorithm proposed here should expand the capability of the previous version in generating higher-order, multivariate orthogonal polynomials for an arbitrary, dependent probability measure of input variables.

For an ith element $\Psi_i(\mathbf{Z};\mathbf{g})$ of the orthonormal polynomial vector $\boldsymbol{\Psi}_m(\mathbf{Z};\mathbf{g}) = (\Psi_1(\mathbf{Z};\mathbf{g}), \ldots, \Psi_{L_{N,m}}(\mathbf{Z};\mathbf{g}))^{\intercal}$, the first- and second-order moments are (Lee and Rahman 2020)

$$\mathbb{E}_{\mathbf{g}}\left[\Psi_i(\mathbf{Z};\mathbf{g})\right] = \begin{cases} 1, & \text{if } i = 1, \\ 0, & \text{if } i \neq 1, \end{cases} \tag{7}$$

and

$$\mathbb{E}_{\mathbf{g}}\left[\Psi_i(\mathbf{Z};\mathbf{g})\Psi_j(\mathbf{Z};\mathbf{g})\right] = \begin{cases} 1, & i = j, \\ 0, & i \neq j, \end{cases} \tag{8}$$

respectively. These properties are essential to GPCE, to be exploited in a forthcoming section.

Note that the above three-step algorithm is described in terms of orthonormal polynomials in $\mathbf{z}$, not $\mathbf{x}$. This is chiefly because $\mathbf{g}$ and hence $\boldsymbol{\Psi}_m(\mathbf{z};\mathbf{g})$ are intended to be invariant when the design vector $\mathbf{d}$ changes during design iterations. To explain this further, consider the qth RBDO subproblem in (5), where the shifting and scaling transformations for the kth initial design variable yield

$$\mathbb{E}_{\mathbf{d}^{\{q\}}}\left[Z_{i_k}\right] = g_k^{\{q\}} = \begin{cases} d_k^{\{q\}} + r_{i_k}^{\{q\}}, & \text{shifting}, \\ d_k^{\{q\}} r_{i_k}^{\{q\}}, & \text{scaling}. \end{cases} \tag{9}$$

For (9), one may choose any value of $g_k^{\{q\}}$ with respect to $d_{k,0}^{\{q\}}$. However, for the sake of convenience, assign $d_{k,0}^{\{q\}}$ to $d_k^{\{q\}}$ and $g_k^{\{q\}}$ to *zero* and *one* in the shifting and scaling transformations, respectively. Then, $r_{i_k}^{\{q\}}$ is determined to be $-d_{k,0}^{\{q\}}$ and $1/d_{k,0}^{\{q\}}$, respectively, from (9). Solving the qth RBDO subproblem with the initial design $\mathbf{d}_0^{\{q\}}$ yields $\mathbf{d}_*^{\{q\}}$. Repeatedly, when updating the process from the qth to $(q+1)$th design iterations, choose the same values of $g_k^{\{q\}}$ to be *zero* and *one* in the shifting and scaling transformations, respectively, for all $q = 1, 2, \ldots, Q$. It contributes to only one sequence of calculation of the measure-consistent orthonormal polynomials $\boldsymbol{\Psi}_m(\mathbf{z};\mathbf{g})$ throughout all design iterations.

3.2 Generalized polynomial chaos expansion

According to (7) and (8), any two distinct elements $\Psi_i(\mathbf{z};\mathbf{g})$ and $\Psi_j(\mathbf{z};\mathbf{g})$, $i,j = 1, \ldots, L_{N,m}$, of the polynomial vector $\boldsymbol{\Psi}_m(\mathbf{z};\mathbf{g})$ are mutually orthonormal with respect to the probability measure of $\mathbf{Z}$. Therefore, the set $\{\Psi_i(\mathbf{z};\mathbf{g}), 1 \le i \le L_{N,m}\}$ from $\boldsymbol{\Psi}_m(\mathbf{z};\mathbf{g})$ is linearly independent. Moreover, the set has the $L_{N,m}$-dimension, which is equal to the dimension of the polynomial space of degree at most m. Hence, as $m \to \infty$, $L_{N,m} \to \infty$ and the resulting set $\{\Psi_i(\mathbf{z};\mathbf{g}), 1 \le i < \infty\}$ comprises an infinite number of basis functions. If the probability measure of random input $\mathbf{Z}$ is compactly supported or is exponentially integrable (Rahman 2018), as assumed here, the set $\{\Psi_i(\mathbf{Z};\mathbf{g}), 1 \le i < \infty\}$ forms an orthonormal basis of $L^2(\Omega_{\mathbf{d}}, \mathcal{F}_{\mathbf{d}}, \mathbb{P}_{\mathbf{d}})$. Therefore, any random variable $h(\mathbf{Z};\mathbf{r}) \in L^2(\Omega_{\mathbf{d}}, \mathcal{F}_{\mathbf{d}}, \mathbb{P}_{\mathbf{d}})$ can be expanded as a Fourier series comprising multivariate orthonormal polynomials in $\mathbf{Z}$, referred to as the GPCE of[1]

$$h(\mathbf{Z};\mathbf{r}) \sim \sum_{i=1}^{\infty} C_i(\mathbf{r})\Psi_i(\mathbf{Z};\mathbf{g}), \tag{10}$$

where the expansion coefficients $C_i \in \mathbb{R}$, $i = 1, \ldots, \infty$, are given by

$$\begin{aligned} C_i(\mathbf{r}) &:= \mathbb{E}_{\mathbf{g}}\left[h(\mathbf{Z};\mathbf{r})\Psi_i(\mathbf{Z};\mathbf{g})\right] \\ &:= \int_{\mathbb{R}^N} h(\mathbf{z};\mathbf{r})\Psi_i(\mathbf{z};\mathbf{g})f_{\mathbf{Z}}(\mathbf{z};\mathbf{g})d\mathbf{z}. \end{aligned} \tag{11}$$

According to (Rahman 2018), the GPCE of $h(\mathbf{Z};\mathbf{r}) \in L^2(\Omega_{\mathbf{d}}, \mathcal{F}_{\mathbf{d}}, \mathbb{P}_{\mathbf{d}})$ converges in mean square, in probability, and in distribution.

[1] Here, the symbol ~ represents equality in a weaker sense, such as equality in mean square, but not necessarily pointwise, nor almost everywhere.

The GPCE involves an infinite number of orthonormal polynomials or coefficients. However, in a practical setting, the number must be finite, meaning that the GPCE must be truncated. There are several ways to truncate the expansion, such as those involving tensor-product, total-degree, and hyperbolic-cross index sets. In this work, the truncation stemming from the total-degree index set is employed, which retains polynomial expansion orders less than or equal to $m \in \mathbb{N}_0$. The result is an mth-order GPCE approximation of $h(\mathbf{Z};\mathbf{r})$, given by

$$h_m(\mathbf{Z};\mathbf{r}) = \sum_{i=1}^{L_{N,m}} C_i(\mathbf{r})\Psi_i(\mathbf{Z};\mathbf{g}), \tag{12}$$

which comprises $L_{N,m}$ expansion coefficients defined by (11).

The GPCE in (10) and (11) should not be confused with that of Xiu and Karniadakis (2002). The GPCE here is meant for an arbitrary dependent probability distribution of random input. On the contrary, the existing PCE, whether classical (Wiener 1938) or generalized (Xiu and Karniadakis 2002), still needs independence of random input.

3.3 Expansion coefficients

The definitions of expansion coefficients of an mth-order GPCE approximation $h_m(\mathbf{Z};\mathbf{r})$ mandate various N-dimensional integrations. For an arbitrary function h and an arbitrary probability distribution of random input $\mathbf{Z}$, their exact evaluations from the definition alone are impractical. Numerical integration entailing a multivariate, tensor-product Gauss-type quadrature rule is computationally intensive, if not prohibitive, for high-dimensional ($N \geq 10$, say) RBDO problems. To resolve this difficulty, standard least squares (SLS) was employed to estimate the coefficients. Here, only a brief summary of SLS is given for the paper to be self-contained. For additional details, readers are advised to consult a related work of Lee and Rahman (2020).

From the known distribution of random input $\mathbf{Z}$ and an output function $h : \bar{\mathbb{A}}^N \to \mathbb{R}$, consider an input–output data set $\{\mathbf{z}^{(l)}, h(\mathbf{z}^{(l)};\mathbf{r})\}_{l=1}^{L}$ of size $L \in \mathbb{N}$, where $\mathbf{r}$ is decided from the knowledge of $\mathbf{d}$ and $\mathbf{g}$, as discussed earlier. The data set, often referred to as the experimental design, is generated by calculating the function h at each input data $\mathbf{z}^{(l)}$. Various sampling methods, namely, standard MCS, quasi-MCS (QMCS), Latin hypercube sampling, can be used to build the experimental design. Using the experimental design, the approximate GPCE coefficients $\tilde{C}_i(\mathbf{d}), i = 1, \ldots, L_{N,m}$, satisfy the linear system

$$\mathbf{A}\mathbf{c} = \mathbf{b},$$

where

$$\begin{aligned} \mathbf{A} &:= \begin{bmatrix} \tilde{\Psi}_1(\mathbf{z}^{(1)};\mathbf{g}) & \cdots & \tilde{\Psi}_{L_{N,m}}(\mathbf{z}^{(1)};\mathbf{g}) \\ \vdots & \ddots & \vdots \\ \tilde{\Psi}_1(\mathbf{z}^{(L)};\mathbf{g}) & \cdots & \tilde{\Psi}_{L_{N,m}}(\mathbf{z}^{(L)};\mathbf{g}) \end{bmatrix}, \\ \mathbf{b} &:= (h(\mathbf{z}^{(1)};\mathbf{r}), \ldots, h(\mathbf{z}^{(L)};\mathbf{r}))^\intercal, \text{ and} \\ \mathbf{c} &:= (\tilde{C}_1(\mathbf{r}), \ldots, \tilde{C}_{L_{N,m}}(\mathbf{r}))^\intercal. \end{aligned} \tag{13}$$

From (13), $\tilde{\Psi}_i(\mathbf{z}^{(l)};\mathbf{g})$ represents an estimate of $\Psi_i(\mathbf{z}^{(l)};\mathbf{r})$ owing to approximations resulting from the construction of the monic moment matrix in Sect. 3.1. According to SLS, the best set of expansion coefficients are estimated by minimizing the mean-squared residual

$$\hat{e}_m := \frac{1}{L}\sum_{l=1}^{L}\left[h(\mathbf{z}^{(l)};\mathbf{r}) - \sum_{i=1}^{L_{N,m}} \tilde{C}_i\tilde{\Psi}_i(\mathbf{z}^{(l)};\mathbf{g})\right]^2. \tag{14}$$

As a result, the SLS solution $\hat{C}_i,\ i = 1, \ldots, L_{N,m}$, is obtained from

$$\mathbf{A}^\intercal\mathbf{A}\hat{\mathbf{c}} = \mathbf{A}^\intercal\mathbf{b},$$

where $\hat{\mathbf{c}} := (\hat{C}_1(\mathbf{r}), \ldots, \hat{C}_{L_{N,m}}(\mathbf{r}))^\intercal$ and the $L_{N,m} \times L_{N,m}$ matrix $\mathbf{A}^\intercal\mathbf{A}$ is referred to as the information or data matrix. Finally, the inversion of the data matrix, if it is positive-definite, produces the best estimate

$$\hat{\mathbf{c}} = (\mathbf{A}^\intercal\mathbf{A})^{-1}\mathbf{A}^\intercal\mathbf{b}$$

of the approximate GPCE coefficients. When using SLS, the number of experimental data must be larger than the number of coefficients, that is, $L > L_{N,m}$. Even if this condition is met, the experimental design must be carefully chosen to ensure that the resulting matrix $\mathbf{A}^\intercal\mathbf{A}$ is well conditioned.

While this paper employs MCS for sampling the input random variables, it is also possible to use an optimal design of experiments (ODE) (Hadigol and Doostan 2018; Luthen et al. 2021). A detailed study entailing such ODEs is beyond the scope of this work.

3.4 Failure probability

The mth-order GPCE $h_m(\mathbf{Z};\mathbf{r})$ can be used as an inexpensive surrogate model that replaces an expensive-to-calculate function $h(\mathbf{Z};\mathbf{r})$. Thus, for reliability analysis of performance functions $h(\mathbf{Z};\mathbf{r})$ in Sect. 2, the estimation of the failure probability can be conducted using MCS of $h_m(\mathbf{Z};\mathbf{r})$, as explained below.

Depending on component or system reliability analysis, let $\bar{\Omega}_{F,m} := \{\mathbf{z} : h_m(\mathbf{z};\mathbf{r}) < 0\}$ or $\bar{\Omega}_{F,m} := \{\mathbf{z} : \cup_i h_{i,m}(\mathbf{z};\mathbf{r}) < 0\}$ or $\{\mathbf{z} : \cap_i h_{i,m}(\mathbf{z};\mathbf{r}) < 0\}$ be a failure set, as a result of the mth-order GPCE $h_m(\mathbf{Z};\mathbf{r})$ of $h(\mathbf{Z};\mathbf{r})$ or $h_{i,m}(\mathbf{Z};\mathbf{r})$ of $h_i(\mathbf{Z};\mathbf{r})$. Then, the GPCE estimate of the failure probability $P_F(\mathbf{d})$ is

$$\begin{aligned}\mathbb{P}_{\mathbf{g}}\left[\mathbf{Z}\in\bar{\Omega}_{F,m}\right] &:= \int_{\bar{\mathbb{A}}^N} I_{\bar{\Omega}_{F,m}}(\mathbf{z};\mathbf{r}) f_{\mathbf{Z}}(\mathbf{z};\mathbf{g})d\mathbf{z}\\ &:= \mathbb{E}_{\mathbf{g}}\left[I_{\bar{\Omega}_{F,m}}(\mathbf{Z};\mathbf{r})\right]\\ &:= \lim_{\bar{L}\to\infty}\frac{1}{\bar{L}}\sum_{l=1}^{\bar{L}} I_{\bar{\Omega}_{F,m}}(\mathbf{z}^{(l)};\mathbf{r}),\end{aligned} \tag{15}$$

where $\mathbf{z}^{(l)}$ is the lth realization of $\mathbf{Z}$, $\bar{L}$ is the sample size, and $I_{\bar{\Omega}_{F,m}}$ is another indicator function such that

$$I_{\bar{\Omega}_{F,m}} = \begin{cases} 1, & \mathbf{z}\in\bar{\Omega}_{F,m},\\ 0, & \mathbf{z}\notin\bar{\Omega}_{F,m}.\end{cases}$$

Note that the MCS of GPCE approximation in (15) should not be confused with crude MCS commonly used for producing benchmark results. The crude MCS, which requires numerical calculations of h or h_i for input samples $\mathbf{z}^{(l)}$, $l=1,\cdots,L$, can be expensive or even prohibitive, particularly when the sample size L needs to be very large for estimating small failure probabilities. In contrast, the MCS embedded in the GPCE approximation requires evaluations of simple polynomial functions that describe h_m or $h_{i,m}$. Therefore, an arbitrarily large sample size can be accommodated in the GPCE approximation.

4 Proposed method for design sensitivity analysis

When solving an RBDO problem with a gradient-based optimization algorithm, such as sequential linear or quadratic programming, at least the first-order derivatives of the failure probability associated with the functions $h_l(\mathbf{Z};\mathbf{r})$, $l=0,1,\ldots,K$, with respect to each design variable d_k, $k=1,\ldots,M$, are required. In this section, an analytical design sensitivity formulation is unveiled by combining the GPCE approximation with score function for dependent input random variables. For such sensitivity analysis, the following regularity conditions are necessary:

1. The PDF $f_{\mathbf{Z}}(\mathbf{z};\mathbf{g})$ of $\mathbf{Z}$ is continuous. Also, the partial derivative $\partial f_{\mathbf{Z}}(\mathbf{z};\mathbf{g})/\partial g_k$, $k=1,\ldots,M$, exists and is finite for all possible values of $\mathbf{z}$ and g_k. Moreover, the failure probability associated with the performance function $h(\mathbf{Z};\mathbf{r})$ is a differentiable function of $\mathbf{g}$.
2. There exists a Lebesgue integrable dominating function $t(\mathbf{z})$ such that

$$\left|I_{\bar{\Omega}_F}(\mathbf{z};\mathbf{r})\frac{\partial f_{\mathbf{Z}}(\mathbf{z};\mathbf{g})}{\partial d_k}\right| \le t(\mathbf{z}),\ k=1,\ldots,M.$$

Note that the sensitivity formulation proposed in the following subsections is new since the existing sensitivity analysis is limited to only independent random variables (Ren et al. 2016).

4.1 Score function

Suppose the first-order derivatives of the failure probability $\mathbb{P}_{\mathbf{g}}\left[\mathbf{Z}\in\bar{\Omega}_F\right]$ corresponding to a generic performance function $h(\mathbf{Z};\mathbf{r})$ with respect to design variables d_k, $k=1,\ldots,M$, have to be computed in solving the qth RBDO subproblem in (5). During the design process of the qth subproblem, $\mathbf{g}^{\{q\}}$ changes, but $\mathbf{r}^{\{q\}}$ remains constant locally. For brevity, the iteration or the subproblem number q is omitted from $\mathbf{d}^{\{q\}}$, $\mathbf{g}^{\{q\}}$, and $\mathbf{r}^{\{q\}}$ in the remainder of this section.

From (6), recall that $\mathbb{P}_{\mathbf{g}}\left[\mathbf{Z}\in\bar{\Omega}_F\right] := \mathbb{E}_{\mathbf{g}}[I_{\bar{\Omega}_F}]$. Then, applying the partial derivative with respect to d_k to $\mathbb{E}_{\mathbf{g}}[I_{\bar{\Omega}_F}]$ and invoking the chain rule and Lebesgue dominated convergence theorem (Browder 1996), which allows one to interchange the differential and integral operators, produces the first-order sensitivities

$$\begin{aligned}\frac{\partial\mathbb{P}_{\mathbf{g}}\left[\mathbf{Z}\in\bar{\Omega}_F\right]}{\partial d_k} &= \frac{\partial\mathbb{E}_{\mathbf{g}}\left[I_{\bar{\Omega}_F}(\mathbf{Z};\mathbf{r})\right]}{\partial d_k}\\ &= \frac{\partial}{\partial d_k}\int_{\bar{\mathbb{A}}^N} I_{\bar{\Omega}_F}(\mathbf{z};\mathbf{r}) f_{\mathbf{Z}}(\mathbf{z};\mathbf{g})d\mathbf{z}\\ &= \frac{\partial g_k}{\partial d_k}\frac{\partial}{\partial g_k}\int_{\bar{\mathbb{A}}^N} I_{\bar{\Omega}_F}(\mathbf{z};\mathbf{r}) f_{\mathbf{Z}}(\mathbf{z};\mathbf{g})d\mathbf{z}\\ &= \frac{\partial g_k}{\partial d_k}\int_{\bar{\mathbb{A}}^N} I_{\bar{\Omega}_F}(\mathbf{z};\mathbf{r})\frac{\partial \ln f_{\mathbf{Z}}(\mathbf{z};\mathbf{g})}{\partial g_k} f_{\mathbf{Z}}(\mathbf{z};\mathbf{g})d\mathbf{z},\\ &\quad k=1,\ldots,M,\end{aligned} \tag{16}$$

where $\partial g_k/\partial d_k$=1 or r_{i_k} for the shifting or scaling transformations, respectively. Define by

$$s_k(\mathbf{Z};\mathbf{g}) := \frac{\partial \ln f_{\mathbf{Z}}(\mathbf{Z};\mathbf{g})}{\partial g_k} \tag{17}$$

the first-order score function (Rahman 2009b; Rubinstein and Shapiro 1993) for the variable g_k. Usually, the score functions can be determined numerically or analytically – for instance, when $\mathbf{Z}$ follows classical probability distributions, such as those obtained for multivariate Gaussian and lognormal density functions in Table 1.

Combining (16) and (17) results in

$$\begin{aligned}\frac{\partial\mathbb{P}_{\mathbf{g}}\left[\mathbf{Z}\in\bar{\Omega}_F\right]}{\partial d_k} &= \frac{\partial g_k}{\partial d_k}\int_{\bar{\mathbb{A}}^N} I_{\bar{\Omega}_F}(\mathbf{z};\mathbf{r}) s_k(\mathbf{z};\mathbf{g}) f_{\mathbf{Z}}(\mathbf{z};\mathbf{g})d\mathbf{z}\\ &= \frac{\partial g_k}{\partial d_k}\mathbb{E}_{\mathbf{g}}\left[I_{\bar{\Omega}_F}(\mathbf{Z};\mathbf{r}) s_k(\mathbf{Z};\mathbf{g})\right],\quad k=1,\ldots,M.\end{aligned} \tag{18}$$

According to (6) and (18), the failure probability and its sensitivities have both been formulated as expectations of stochastic quantities with respect to the same probability

Table 1 Derivatives of log-density functions for two types of multivariate distributions (Lee and Rahman 2021)

Type	Score function for design variables $\mathbf{g} = (g_1, \dots, g_M)$.
	Gaussian density on $(-\infty, \infty)^N$
1	$s_k(\mathbf{z};\mathbf{g})^{(a)} = \sum_{j=1}^{N} p_{i_k j}(z_j - \mu_j)$,
	$\mu_{i_k} = g_k, k = 1, \dots, M, 1 \le i_1 < \cdots < i_M \le N$,
	$[p_{i,j}] = \boldsymbol{\Sigma}_{\mathbf{Z}}^{-1} \in \mathbb{R}^{N\times N}$, $\boldsymbol{\Sigma}_{\mathbf{Z}} = [\rho_{ij}\sigma_i\sigma_j]$,
	$0 < \sigma_i < \infty, -1 < \rho_{ij} < 1, i, j = 1, \dots, N$.
	Lognormal density on $[0, \infty)^N$
2	$s_k(\mathbf{z};\mathbf{g})^{(a)} = l_k \sum_{j=1}^{N} \tilde{p}_{i_k j}(\ln z_j - \tilde{\mu}_j)^{(b)}$,
	$\tilde{\mu}_i = \ln[\mu_i^2 \,/\, \sigma_i] - 1 \,/\, 2$, $\tilde{\sigma}_i = \sqrt{\ln\left[\sigma_i^2 \,/\, \mu_i^2\right] + 1}$,
	$\mu_{i_k} = g_k, k = 1, \dots, M, 1 \le i_1 < \cdots < i_M \le N$,
	$[\tilde{p}_{i,j}] = \tilde{\boldsymbol{\Sigma}}_{\ln\mathbf{Z}}^{-1} \in \mathbb{R}^{N\times N}$, $\tilde{\boldsymbol{\Sigma}}_{\ln\mathbf{Z}} = [\tilde{\rho}_{ij}\tilde{\sigma}_i\tilde{\sigma}_j]$,
	$\tilde{\rho}_{ij} = \ln\left[\rho_{ij} \,/\, (\mu_i\mu_j) + 1\right] \,/\, (\tilde{\sigma}_i\tilde{\sigma}_j)$,
	$0 < \sigma_i < \infty, -1 < \rho_{ij} < 1, i, j = 1, \dots, N$.

a. $s_k(\mathbf{z};\mathbf{g}) = \partial \ln f_{\mathbf{Z}}(\mathbf{z};\mathbf{g}) \,/\, \partial g_k$

b. $l_k = [1 + 2(\sigma_{i_k}/g_k)^2] \,/\, [g_k\{1 + (\sigma_{i_k}/g_k)^2\}]$

measure, facilitating their concurrent evaluations in a single stochastic simulation or analysis.

4.2 Sensitivity analysis

In general, the sensitivities of failure probability are not available analytically, since the failure probability is not either. The main contribution of this work is to simultaneously estimate both the failure probability and its sensitivity by GPCE, providing a computationally efficient, alternative route to the traditional MCS.

Replacing $h(\mathbf{z};\mathbf{r})$ with its mth-order GPCE approximation $h_m(\mathbf{z};\mathbf{r})$, the resultant approximation of the sensitivities of the failure probability is obtained as

$$\begin{aligned}\frac{\partial \mathbb{P}_{\mathbf{g}}\left[\mathbf{Z} \in \bar{\Omega}_{F,m}\right]}{\partial d_k} &= \frac{\partial \mathbb{E}_{\mathbf{g}}[I_{\bar{\Omega}_{F,m}}(\mathbf{Z};\mathbf{r})]}{\partial d_k} \\ &= \frac{\partial g_k}{\partial d_k}\mathbb{E}_{\mathbf{g}}\left[I_{\bar{\Omega}_{F,m}}(\mathbf{Z};\mathbf{r})s_k(\mathbf{Z};\mathbf{g})\right] \\ &= \frac{\partial g_k}{\partial d_k}\lim_{\bar{L}\to\infty}\frac{1}{\bar{L}}\sum_{l=1}^{\bar{L}}\left[I_{\bar{\Omega}_{F,m}}(\mathbf{z}^{(l)})s_k(\mathbf{z}^{(l)};\mathbf{g})\right],\end{aligned} \tag{19}$$

where $\bar{L}$ is the sample size and $\mathbf{z}^{(l)}$ is the lth realization of $\mathbf{Z}$. The sensitivity in (19) is easily and inexpensively determined by sampling elementary polynomial functions that describe $h_m(\mathbf{Z};\mathbf{r})$ in (12) and $s_k(\mathbf{Z};\mathbf{g})$ in (17) using MCS. The same input data set $\{\mathbf{z}^{(l)}\}_{l=1}^{\bar{L}}$ of size $\bar{L} \in \mathbb{N}$ used to calculate the failure probability in Sect. 3.4 can be employed for such sensitivity analysis. Furthermore, during design iterations, $\mathbf{z}$ and $\mathbf{g}$ are fixed, thereby avoiding recalculations of $s_k(\mathbf{z};\mathbf{g})$. However, $h_m(\mathbf{z};\mathbf{r})$ is required to be recalculated as $\mathbf{r}$ changes during design iterations. Having said so, these recalculations can also be circumvented using a single-step design process, to be introduced in Sect. 5.2.

The GPCE coefficients depend on $\mathbf{g}$. Naturally, a GPCE approximation, whether obtained by truncating arbitrarily or adaptively, is also dependent on $\mathbf{g}$, unless the approximation exactly reproduces the function h. It is important to clarify that the approximate sensitivity in (19) is obtained not by taking partial derivatives of the approximate failure probability in (15) with respect to g_k. Instead, it results from replacing h with h_m in the expectation describing the last line of (18).

The incorporation of score functions has the desirable property that it requires differentiating only the underlying PDF $f_{\mathbf{Z}}(\mathbf{z};\mathbf{g})$. The resulting score functions can be easily and, in most cases, analytically determined. If the performance function is not differentiable or discontinuous—for example, the indicator function that comes from reliability analysis—the proposed method still allows evaluation of the sensitivity if the density function is differentiable. In reality, the density function is often smoother than the performance function, and therefore the proposed sensitivity methods are able to calculate sensitivities for a wide variety of complex mechanical systems.

5 Proposed method for RBDO

The GPCE approximations, described in the foregoing sections, are intended to evaluate the constraint functions $c_l(\mathbf{d})$, $l = 1, \dots, K$, and its design sensitivities from a single stochastic analysis. Such approximation, in contrast, is not demanded when the objective function is a simple and explicit deterministic mapping between design variables and output. However, it is conceivable that the objective function may also be defined as the statistical mean of a response function of random variables whose distribution parameters are specified by design variables $\mathbf{d} = (d_1, \dots, d_M)^{\intercal}$. For instance, let $h_0(\mathbf{z};\mathbf{r}) \in L^2(\Omega_{\mathbf{d}}, \mathcal{F}_{\mathbf{d}}, \mathbb{P}_{\mathbf{d}})$ be a random output function of an input random vector $\mathbf{z} := (z_1, \dots, z_N)^{\intercal}$ with known PDF $f_{\mathbf{Z}}(\mathbf{z};\mathbf{g})$. Then, the objective function in (4) can be generalized to read

$$c_0(\mathbf{d}) := \mathbb{E}_{\mathbf{g}(\mathbf{d})}[h_0(\mathbf{Z};\mathbf{r})],$$

where $\mathbb{E}_{\mathbf{g}(\mathbf{d})}[h_0(\mathbf{Z};\mathbf{r})] := \int_{\mathbb{R}^N} h_0(\mathbf{z};\mathbf{r})f_{\mathbf{Z}}(\mathbf{z};\mathbf{g}(\mathbf{d}))d\mathbf{z}$. In this case, the objective function and its design sensitivities can also be evaluated by a similar combination of GPCE approximation and score functions, as briefly summarized in Appendices 1 and 2. Readers interested in additional details, including general statistical moment and design sensitivity analyses by GPCE, are directed to the authors' prior work on RDO (Lee and Rahman 2021).

An integration of reliability analysis, design sensitivity analysis, and a suitable optimization algorithm is expected to yield a convergent solution of an RBDO problem defined in (4). However, new reliability and sensitivity analyses through recalculations of the GPCE expansion coefficients are demanded at every design iteration. In addition, if the objective and/or constraint functions are highly nonlinear, there is a need for high-order GPCE approximations valid for the entire design space, leading to a computationally intensive design process. In such cases, GPCE with a low-order approximation may not even find the correct optimal solution. Therefore, a straightforward integration is costly, depending on the expense of evaluating the objective and constraint functions and the requisite number of design iterations. To resolve these problems, a multi-point design process (Ren et al. 2016) featuring sequential formulations of local RBDO problems through a single-step process with GPCE approximations is presented to efficiently obtain a convergent solution of the original RBDO problem.

5.1 Multi-point approximation

The multi-point approximation entails local implementations of the GPCE approximation that are built on subregions of the entire design space. According to this method, the original RBDO problem is exchanged with a series of local RBDO problems, where the objective and constraint functions in each local RBDO problem represent their multi-point approximations (Toropov et al. 1993).

For the rectangular design space

$$\mathcal{D} = \times_{k=1}^{k=M}[d_{k,L}, d_{k,U}] \subseteq \mathbb{R}^M$$

of the RBDO problem described in (4), denote by $q' = 1, 2, \ldots, Q'$, $Q' \in \mathbb{N}$, an index indicating the q'th subregion of $\mathcal{D}$ with the initial design vector $\mathbf{d}_0^{(q')} = (d_{1,0}^{(q')}, \ldots, d_{M,0}^{(q')})^\intercal$. Given a sizing factor $0 < \beta_k^{(q')} \le 1$, the domain of the q'th subregion is expressed by

$$\begin{aligned}\mathcal{D}^{(q')} = \times_{k=1}^{k=M}\Bigg[&d_{k,0}^{(q')} - \beta_k^{(q')}\frac{(d_{k,U} - d_{k,L})}{2},\\ &d_{k,0}^{(q')} + \beta_k^{(q')}\frac{(d_{k,U} - d_{k,L})}{2}\Bigg] \subseteq \mathcal{D} \subseteq \mathbb{R}^M,\\ &q' = 1, \ldots, Q'.\end{aligned}$$

According to the multi-point design process, the RBDO problem in (4) is transformed to a succession of local RBDO problems for Q' subregions. For the q'th subregion, the local RBDO problem requires one to

$$\begin{aligned}&\min_{\mathbf{d}\in\mathcal{D}^{(q')}\subseteq\mathbb{R}^M} \tilde{c}_{0,m}^{(q')}(\mathbf{d})\\ &\text{subject to } \tilde{c}_{l,m}^{(q')}(\mathbf{d}) := \mathbb{P}_{\mathbf{g}}[\mathbf{Z} \in \tilde{\bar{\Omega}}_{F,l,m}^{(q')}(\mathbf{d})] - p_l \le 0,\\ &d_k \in \left[d_{k,0}^{(q')} - \beta_k^{(q')}(d_{k,U} - d_{k,L})\,/\,2,\right.\\ &\left.d_{k,0}^{(q')} + \beta_k^{(q')}(d_{k,U} - d_{k,L})\,/\,2\right],\\ &l = 1, \ldots, K;\ k = 1, \ldots, M,\end{aligned} \tag{20}$$

where $\tilde{c}_{0,m}^{(q')}$, $\tilde{\bar{\Omega}}_{F,l,m}^{(q')}(\mathbf{d})$, and $\tilde{c}_{l,m}^{(q')}(\mathbf{d})$, $l = 1, \ldots, K$, are the mth-order GPCE approximations of, respectively, $c_0(\mathbf{d})$, $\bar{\Omega}_{F,l}(\mathbf{d})$, and $c_l(\mathbf{d})$ for the q'th subregion problem, and $\tilde{\bar{\Omega}}_{F,l,m}^{(q')}(\mathbf{d})$ is also defined using the mth-order GPCE approximation of $\tilde{h}_{l,m}^{(q')}(\mathbf{z};\mathbf{r})$ of $h_l(\mathbf{z})$, and $d_{k,0}^{(q')} - \beta_k^{(q')}(d_{k,U} - d_{k,L})\,/\,2$ and $d_{k,0}^{(q')} + \beta_k^{(q')}(d_{k,U} - d_{k,L})\,/\,2$, the so-called move limits, are the lower and upper bounds, respectively, of the kth coordinate of the subregion $\mathcal{D}^{(q')}$.

In addition, if the objective function is defined as the mean, that is, $c_0(\mathbf{d}) := \mathbb{E}_{\mathbf{g}(\mathbf{d})}[h_0(\mathbf{Z};\mathbf{r})]$, then its q'th local version becomes

$$\tilde{c}_{0,m}^{(q')}(\mathbf{d}) := \mathbb{E}_{\mathbf{g}(\mathbf{d})}[h_{0,m}^{(q')}(\mathbf{Z};\mathbf{r})], \tag{21}$$

where $\mathbb{E}_{\mathbf{g}(\mathbf{d})}[\tilde{h}_{0,m}^{(q')}(\mathbf{Z};\mathbf{r})] := \int_{\mathbb{A}^N} \tilde{h}_{0,m}^{(q')}(\mathbf{z};\mathbf{r}) f_{\mathbf{Z}}(\mathbf{z};\mathbf{g}(\mathbf{d}))d\mathbf{z}$. From (20) and (21), the iterations with respect to q' are associated with solving local RBDO problems and should not be confused with q describing design iterations or the qth subproblem in (5).

5.2 Single-step process

The single-step process is intended to solve the local RBDO problem in (20) from a single stochastic analysis by obviating the need for recalculation of the GPCE coefficients from a new input–output data set in every design iteration. However, it is predicated on two important assumptions: (1) an mth-order GPCE approximation $h_m(\mathbf{Z};\mathbf{r})$ of $h(\mathbf{Z};\mathbf{r})$ at the initial design is adequate for all possible designs; and (2) the GPCE coefficients for a new design, derived by recycling those for an old design, are acceptable for their accuracy.

Under these two assumptions, let vectors $\mathbf{r}$ and $\mathbf{r}'$ represent the old and new designs, respectively. Assume that GPCE coefficients $C_i(\mathbf{r})$, $i = 1, \ldots, L_{N,m}$, for the old design $\mathbf{r}$ have been already estimated from the old input–output data $\{\mathbf{z}^{(l)}, h(\mathbf{z}^{(l)};\mathbf{r})\}_{l=1}^{L}$. Then, GPCE coefficients $C_i(\mathbf{r}')$, $i = 1, \ldots, L_{N,m}$, for the new design $\mathbf{r}'$ are determined by adjusting the input data set $\{\mathbf{z}^{(l)}\}_{l=1}^{L}$ to the following one $\{\mathbf{z}'^{(l)}\}_{l=1}^{L}$, as

$$\mathbf{z}'^{(l)} = \begin{cases}\mathbf{z}^{(l)} - \mathbf{r}' + \mathbf{r}, & \text{in shifting,}\\ \operatorname{diag}\left(\dfrac{r_1}{r'_1}, \ldots, \dfrac{r_N}{r'_N}\right)\mathbf{z}^{(l)}, & \text{in scaling.}\end{cases}$$

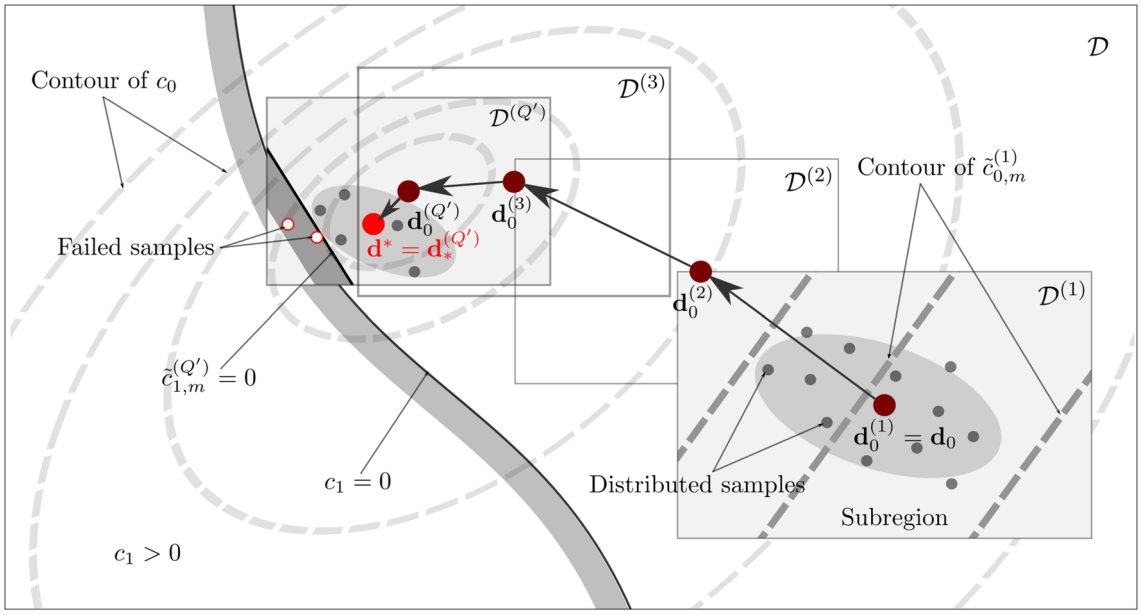

Fig. 2 A schematic description of the multi-point single-step design process during Q' iterations to get the final optimum $\mathbf{d}^*$

To explain the adjustment of input data, first consider the shifting transformation. In this case, the new output value at the lth input sample is

$$h(\mathbf{z}^{(l)};\mathbf{r}') := y(\mathbf{z}^{(l)} - \mathbf{r}') = y(\mathbf{z}^{(l)} - \mathbf{r}' + \mathbf{r} - \mathbf{r}) = y(\mathbf{z}'^{(l)} - \mathbf{r}) =: h(\mathbf{z}'^{(l)};\mathbf{r}),$$

where $\mathbf{z}'^{(l)} := \mathbf{z}^{(l)} - \mathbf{r}' + \mathbf{r}$ is the adjusted lth input sample. Second, for the scaling transformation, the new output value at the lth input sample is

$$\begin{aligned} h(\mathbf{z}^{(l)};\mathbf{r}') &:= y\left(\operatorname{diag}\left[\frac{1}{r_1'},\ldots,\frac{1}{r_N'}\right]\mathbf{z}^{(l)}\right) \\ &= y\left(\operatorname{diag}\left[\frac{1}{r_1},\ldots,\frac{1}{r_N}\right]\right. \\ &\quad \left.\times \operatorname{diag}\left[\frac{r_1}{r_1'},\ldots,\frac{r_N}{r_N'}\right]\mathbf{z}^{(l)}\right) \\ &= y\left(\operatorname{diag}\left[\frac{1}{r_1},\ldots,\frac{1}{r_N}\right]\mathbf{z}'^{(l)}\right) =: h(\mathbf{z}'^{(l)};\mathbf{r}), \end{aligned}$$

where $\mathbf{z}'^{(l)} := \operatorname{diag}[r_1/r_1',\ldots,r_N/r_N']\mathbf{z}^{(l)}$ is the adjusted lth input sample. These adjustments are meant to construct an input–output data set for new designs from GPCE coefficients $C_i(\mathbf{r})$ for the old design, that is,

$$h(\mathbf{z}^{(l)};\mathbf{r}') = h(\mathbf{z}'^{(l)};\mathbf{r}) \approx \sum_{i=1}^{L_{N,m}} C_i(\mathbf{r})\Psi_i(\mathbf{z}'^{(l)};\mathbf{g}), \tag{22}$$

where the last term indicates the mth-order GPCE approximation. Applying (22) to (14) yields an estimate of the mean-square residual

$$\hat{e}_m'' := \frac{1}{L}\sum_{l=1}^{L}\left[\sum_{i=1}^{L_{N,m}} C_i(\mathbf{r})\Psi_i(\mathbf{z}'^{(l)};\mathbf{g}) - \sum_{i=1}^{L_{N,m}} C_i(\mathbf{r}')\Psi_i(\mathbf{z}^{(l)};\mathbf{g})\right]^2, \tag{23}$$

the minimization of which by SLS produces the best estimates of GPCE coefficients for the new design. Compared with the minimization of $\hat{e}_m'$ in (14), the calculation of new output data using the original performance function $h(\mathbf{z}^{(l)};\mathbf{r}')$ is not demanded. Instead, the new output data are estimated by recycling the old coefficients and calculating basis function values at the adjusted input data $\mathbf{z}'$, as shown in (23). Subsequently, new failure probability and design sensitivity analyses, both employing mth-order GPCE approximations from the initial design, are conducted with little extra cost during all design iterations. Therefore, the single-step process holds the potential for substantially lessening the computational effort in solving RBDO problems.

5.3 Multi-point single-step process

When combining the multi-point approximation and the single-step process, the resulting method is equipped to efficiently yield a reliable design solution in solving an RBDO problem defined in (4). The multi-point single-step process is schematically depicted in Fig. 2. Here, $\mathbf{d}_*^{(q')}$ is the optimal design solution obtained using the single-step process for the q'th local RBDO problem in (20). Setting the initial design $\mathbf{d}_0^{(q'+1)}$ to $\mathbf{d}_*^{(q')}$ for the next local RBDO

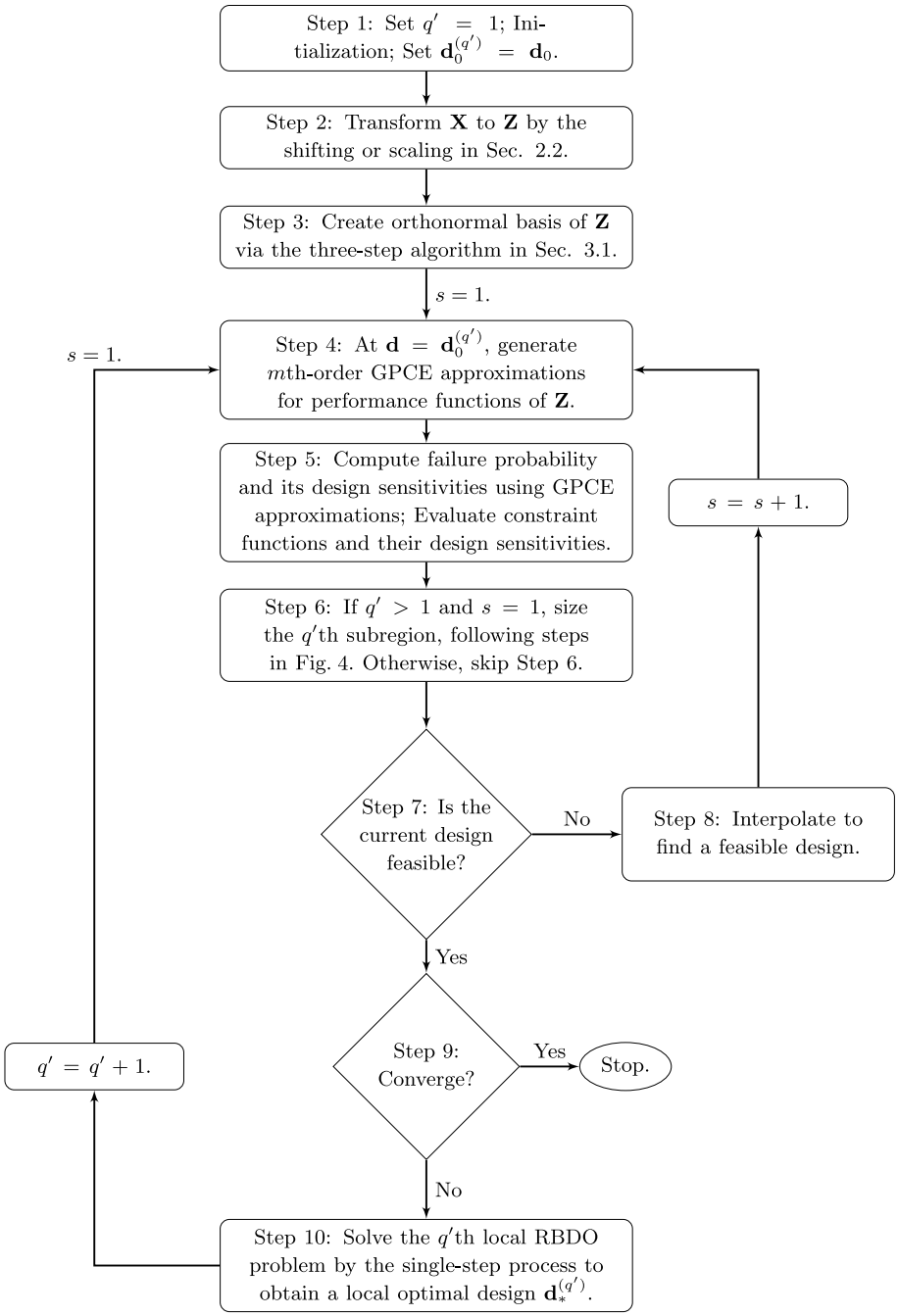

Fig. 3 A flow chart of the MPSS-GPCE method

problem on $\mathcal{D}^{(q'+1)}$, the process is repeated until attaining a final, convergent solution $\mathbf{d}^*$ that satisfies all probabilistic constraints. The flow chart of the method, referred to as the multi-point single-step GPCE or MPSS-GPCE method, is presented in Figs. 3 and 4 with supplementary explanations of each step of the method, as follows.

1. Set termination criteria $0 < \epsilon_1, \epsilon_2 << 1$; set tolerances for sizing subregions $0 < \epsilon_3, \epsilon_4, \epsilon_5, \epsilon_6, \epsilon_7 < 1$; initialize size parameters $0 < \beta_k^{(q')} \leq 1,\ k = 1, \ldots, M$, of $\mathcal{D}^{(q')}$; and set an initial design vector $\mathbf{d}_0^{(q')} = (d_{1,0}^{(q')}, \ldots, d_{M,0}^{(q')})^\intercal$. The initial design can be in either feasible or infeasible domains with respect to the probabilistic constraints.
2. Transform the input random vector $\mathbf{X}$ to a new random vector $\mathbf{Z}$ such that $\mathbb{E}_{\mathbf{d}}[Z_{i_k}] = g_k = 0$ or $1, k = 1, \ldots, M$, by shifting or scaling, respectively, described in Sect. 2.2.
3. Select the total degree $m \in \mathbb{N}$ of GPCE approximations for performance functions $h_l(\mathbf{z};\mathbf{r}), l = 1, \ldots, K$. Construct an $L_{N,m}$-dimensional vector of measure con-

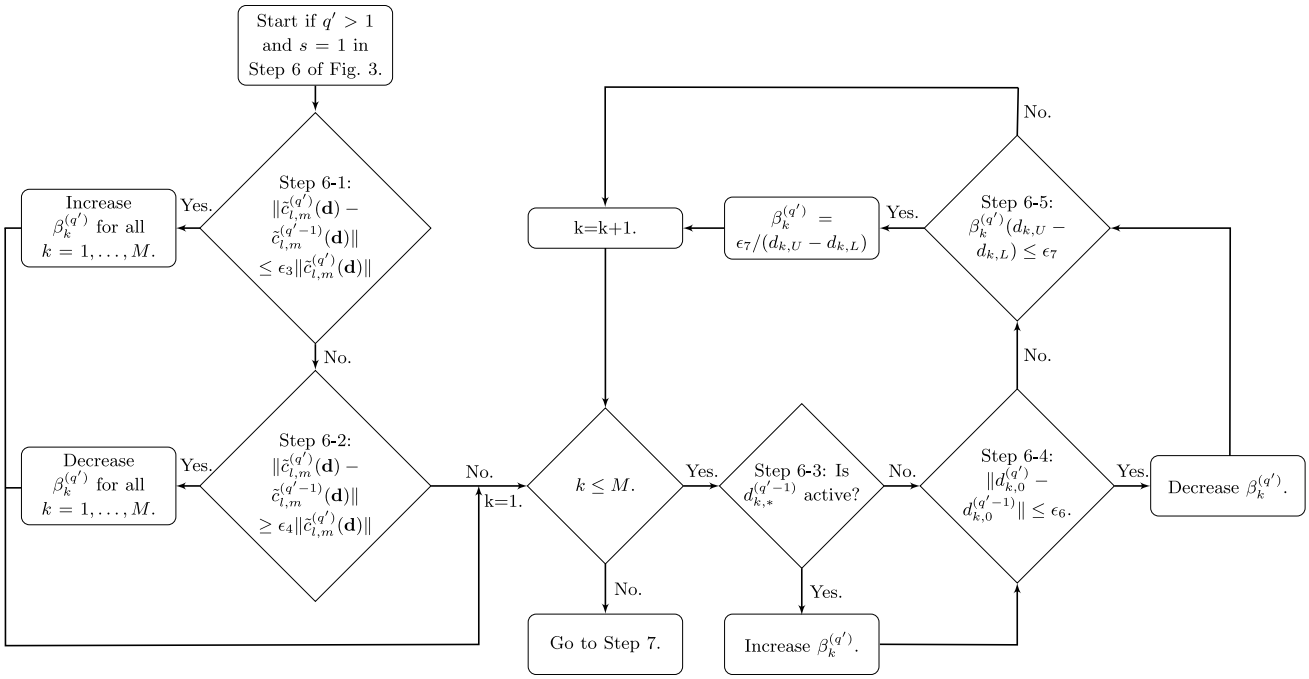

Fig. 4 A flow chart of sizing the q'th subregion in the multi-point single-step design process

sistent orthonormal polynomials $\mathbf{\Psi}_m(\mathbf{Z};\mathbf{g})$ through the three-step algorithm, described in Sect. 3.1.

4. Update the current design vector $\mathbf{d}$, as follows. If $q' = 1$, create input samples $\mathbf{z}^{(l)}$, $l = 1, \ldots, \bar{L}$, where $\bar{L} >> L$, via the MCS or other experimental design method. Use part of the input samples to construct an input–output data set $\{\mathbf{z}^{(l)}, h(\mathbf{z}^{(l)};\mathbf{r})\}_{l=1}^{L}$ of sample size $L > L_{N,m}$ (say, $L/L_{N,m} \ge 3$). If $q' > 1$, reuse the input samples to generate new input–output data sets $\{\mathbf{z}^{(l)}, h(\mathbf{z}^{(l)};\mathbf{r}')\}_{l=1}^{L}$. In every q' step, use SLS to estimate GPCE coefficients with respect to $\mathbf{\Psi}_m(\mathbf{z};\mathbf{g})$ for a performance function h.
5. In each iteration, conduct reliability analysis and compute the sensitivity of the failure probability with respect to design variables d_k, $k = 1, \ldots, M$, both using mth-order GPCE approximations. For the design sensitivity analysis, if $q' = 1$, construct an input–output data set for score functions, $\{\mathbf{z}^{(l)}, s_k(\mathbf{z}^{(l)};\mathbf{g})\}_{l=1}^{\bar{L}}$, $k = 1, \ldots, M$. Otherwise, reuse the input–output data set created in $q' = 1$. Finally, obtain the constraint function values and its gradients at $\mathbf{d} = \mathbf{d}_0^{(q')}$.
6. If $q' = 1$ and $s = 1$, use the initial or default values of size parameters $0 < \beta_k^{(q')} \le 1$, $k = 1, \ldots, M$, in Step 1. If $q' > 1$ and $s = 1$, modify the size parameters according to three criteria: (1) the accuracy of GPCE approximations, (2) the active/inactive condition of subregion boundaries, and (3) the converging condition of current designs. Otherwise, skip Step 6. The details of the three conditions mentioned earlier are explained in the following steps.

6-1. First condition: For any of $l = 1, \ldots, K$, if $||\tilde{c}_{l,m}^{(q')}(\mathbf{d}_0^{(q')}) - \tilde{c}_{l,m}^{(q'-1)}(\mathbf{d}_0^{(q')})|| \le \epsilon_3 ||\tilde{c}_{l,m}^{(q')}(\mathbf{d}_0^{(q')})||$, increase $\beta_k^{(q')}$ for all $k = 1, \ldots, M$. Otherwise, go to Step 6-2. One may need to control the enlargement rate, depending on the problems at hand. For instance, set $\beta_k^{(q')} = (2 - 1/\phi)\beta_k^{(q'-1)}$, where the golden ratio $\phi \approx 1.618$.

6-2. First condition: For any $l = 1, \ldots, K$, if $||\tilde{c}_{l,m}^{(q')}(\mathbf{d}_0^{(q')}) - \tilde{c}_{l,m}^{(q'-1)}(\mathbf{d}_0^{(q')})|| \ge \epsilon_4 ||\tilde{c}_{l,m}^{(q')}(\mathbf{d}_0^{(q')})||$, decrease $\beta_k^{(q')}$ for all $k = 1, \ldots, M$. As an instance of the decrement rate, set $\beta_k^{(q')} = \beta_k^{(q'-1)}/\phi$, where the golden ratio $\phi \approx 1.618$. Otherwise, go to Step 6-3.

6-3. Second condition: If $d_{k,*}^{(q'-1)}$ is active, increase $\beta_k^{(q')}$, $k = 1, \ldots, M$. Here, the active $d_{k,*}^{(q'-1)}$ means that for $0 < \epsilon_5 < 1$, $||d_{k,*}^{(q'-1)} - d_{k,U}|| \le \epsilon_5$ or $||d_{k,*}^{(q'-1)} - d_{k,L}|| \le \epsilon_5$. As an instance of the enlargement rate, set $\beta_k^{(q')} = (2 - 1/\phi)\beta_k^{(q'-1)}$, where the golden ratio $\phi \approx 1.618$. Otherwise, go to Step 6-4.

6-4. Third condition: If $||d_{k,0}^{(q')} - d_{k,0}^{(q'-1)}|| \le \epsilon_6$, decrease $\beta_k^{(q')}$, $k = 1, \ldots, M$. As an instance of the decrement rate, set $\beta_k^{(q')} = \beta_k^{(q'-1)}/\phi$, where the golden ratio $\phi \approx 1.618$. Otherwise, go to Step 6-5.

6-5. Move limit: If $\beta_k^{(q')}(d_{k,U} - d_{k,L}) < \epsilon_7$, set $\beta_k^{(q')} = \epsilon_7/(d_{k,U} - d_{k,L})$. Otherwise, $k = k + 1$ and repeat the process until the loop condition $k \le M$ is satisfied.

7. If the current design $\mathbf{d}$ is not feasible, that is, at least one constraint is violated, go to Step 8. Otherwise, set $\mathbf{d}$ to the current feasible design $\mathbf{d}_f^{(q')}$, then go to Step 9.
8. Interpolate between the current design $\mathbf{d}$ and the previous feasible design $\mathbf{d}_f^{(q'-1)}$. For instance, set $\mathbf{d} = \mathbf{d}_f^{(q'-1)}/\phi + (1 - 1/\phi)\mathbf{d}$, where the golden ratio $\phi \approx 1.618$. If an initial design at $q' = 1$ is infeasible, interpolate it with upper or lower bounds of the design space, or another initial guess, depending on the problems at hand.
9. If any of the two termination conditions, such that (1) $\|\mathbf{d}_f^{(q')} - \mathbf{d}_f^{(q'-1)}\| \le \epsilon_1$ and/or (2) $\|\tilde{c}_{0,m}^{(q')}(\mathbf{d}_f^{(q')}) - \tilde{c}_{0,m}^{(q')}(\mathbf{d}_f^{(q'-1)})\| \le \epsilon_2$, are met, terminate the optimization process and set the final optimal design as $\mathbf{d}^* = \mathbf{d}_f^{(q')}$. Otherwise, go to Step 10.
10. Solve the q'th local RBDO problem with the single-step process using a gradient-based algorithm, such as sequential quadratic programming, to obtain a local optimal solution $\mathbf{d}_*^{(q')}$. Then, increase the subregion count as $q' = q' + 1$. Set $\mathbf{d}_0^{(q')} = \mathbf{d}_*^{(q'-1)}$ and go to Step 4.

The multi-point single-step GPCE method will be referred to as the MPSS-GPCE method for the remainder of this paper

6 Numerical examples

Four numerical examples are presented to illustrate the proposed MPSS-GPCE method for solving RBDO problems. The objective and constraint functions are either elementary mathematical functions or derived from a simple truss or a more complex, industrial-scale mechanical system. Both size and shape design problems in the context of RBDO were solved. In all examples, the design variables are the statistical means of some or all input random variables following dependent probability distributions.

In the probabilistic constraints of Examples 1–4, all the target probabilities of failure are set to $\Phi(-3) \approx 1.35 \times 10^{-3}$, where $\Phi(\cdot)$ is the standard normal distribution function. Each component of the M-dimensional vector $\mathbf{g}$ is either *zero* or *one*, depending on the shifting or scaling transformations, respectively, for input random variables. The multivariate orthonormal polynomials consistent with the probability measure of $\mathbf{z}$ were determined using the three-step algorithm. The monic moment matrix $\mathbf{G}_m$, constructed from monic polynomial basis, was estimated by QMCS with 5×10^6 samples together with the Sobol sequence (Lee and Rahman 2020). The order (m) of GPCE approximations and sample sizes L and $\bar{L}$ depend on the examples and are listed in Table 2. The GPCE coefficients are estimated using SLS and QMCS-generated input–output data. For reliability and design sensitivity analyses, the input samples $\mathbf{z}^{(l)}$, $l = 1, \ldots, \bar{L}$, were created by MCS for simulation of GPCE approximations.

In Examples 1–3, the objective functions are deterministic, and their design sensitivities were derived analytically. In Example 4, the objective function is the statistical mean of the volume of a jet engine compressor blade root, which is computed by an implicit function from CAD. The mean and its design sensitivities were simultaneously determined employing GPCE approximations, which are explained in Appendices 1 and 2.

As a gradient-based optimization, the sequential quadratic programming was employed to solve RBDO problems in all examples. For the multi-point single-step design process, the tolerances and initial size parameter are as follows: $\epsilon_1 = 1 \times 10^{-3}$, $\epsilon_2 = 1 \times 10^{-3}$, $\epsilon_3 = 0.01$, $\epsilon_4 = 0.07, \epsilon_5 = 0.01, \epsilon_6 = 0.5, \epsilon_7 = 0.05, \epsilon_8 = 1 \times 10^{-4}$, and $\beta_k^{(1)} = 0.3,\ k = 1, \ldots, M$, in all examples.

All numerical results were generated using MATLAB (MATLAB 2019), CREO parametric (CREO 2016), and ABAQUS (ABAQUS 2019) on an Intel Core i7-7700K 4.20 GHz process with 64 GB of RAM.

6.1 Example 1: Optimization involving mathematical functions

Consider a mathematical optimization problem, formerly studied by Noh et al. (2009), involving a two-dimensional Gaussian random vector $\mathbf{X} = (X_1, X_2)^\intercal$. The random variables follow a bivariate Gaussian distribution with means $\mathbb{E}_{\mathbf{d}}[X_1] = d_1$, $\mathbb{E}_{\mathbf{d}}[X_2] = d_2$, standard deviations of 0.3 for X_1 and X_2, and three distinct cases of correlation coefficient between X_1 and X_2: 0.4 (Case 1), −0.4 (Case 2), and 0 (Case 3). The third case of *zero* correlation coefficient indicates statistical independence between X_1 and X_2. Given a design vector $\mathbf{d} = (d_1, d_2)^\intercal$, the objective of this RBDO problem is to

$$\begin{aligned} &\min_{\mathbf{d}\in\mathcal{D}} c_0(\mathbf{d}) := -d_1 + d_2, \\ &\text{subject to } c_l(\mathbf{d}) := \mathbb{P}_{\mathbf{d}}[y_l(\mathbf{X}) \le 0)] - \Phi(-3) \le 0, \\ &0 \le d_1 \le 10,\ 0 \le d_2 \le 10,\ l = 1 - 3, \end{aligned}$$

where

$$y_1(\mathbf{X}) = -1 + \frac{X_1^2 X_2}{20},$$

$$y_2(\mathbf{X}) = -1 + \frac{(X_1 + X_2 - 5)^2}{30} + \frac{(X_1 - X_2 - 12)^2}{120},$$

and

Table 2 The list of parameters (Examples 1–4): GPCE orders (m) and sample sizes (L, $\bar{L}$)

Example 1						
$m^{(a)}$			$L^{(b)}$			$\bar{L}^{(c)}$
y_1	y_2	y_3	y_1	y_2	y_3	–
3	3	3	30	30	30	1, 000, 000
4	4	4	45	45	45	1, 000, 000
Example 2						
$m^{(a)}$			$L^{(b)}$			$\bar{L}^{(c)}$
y_1	y_2	y_3	y_1	y_2	y_3	–
4	4	4	210	210	210	1, 000, 000
5	5	5	378	378	378	1, 000, 000
6	6	6	630	630	630	1, 000, 000
Example 3						
$m^{(a)}$			$L^{(b)}$			$\bar{L}^{(c)}$
y_1	y_2		y_1	y_2		–
2	2		759	759		3, 000, 000
Example 4						
$m^{(d)}$			$L^{(e)}$			$\bar{L}^{(c)}$
y_0	y_1	y_2	y_0	y_1	y_2	3, 000, 000
1	1	1	75	75	75	3, 000, 000

[a]The degree of GPCE approximation for an output response $y_l,\ l = 1, \ldots, K,\ 1 \le K < \infty$

[b]The sample size of input–output data set for expansion coefficients of an output response $y_l,\ l = 1, \ldots, K,\ 0 \le K < \infty$

[c]The sample size of input–output data set for reliability analysis

[d]The degree of GPCE approximation for an output response $y_l,\ l = 0, 1, 2$

[e]The sample size of input–output data set for expansion coefficients of an output response $y_l,\ l = 0, 1, 2$

$$y_3(\mathbf{X}) = -1 + \frac{80}{(X_1^2 + 8X_2 + 5)}$$

are three nonlinear random performance functions of X_1 and X_2. The design vector is $\mathbf{d} \in \mathcal{D}$, where $\mathcal{D} = [0, 10] \times [0, 10] \subset \mathbb{R}^2$. For each case of a correlation coefficient, three different initial designs, such as $(5, 5)^\intercal$, $(1, 1)^\intercal$, and $(9, 4)^\intercal$, were selected to verify the robustness of the proposed method in attaining optimal design solutions.

Using the shifting transformation for input random variables, the proposed MPSS-GPCE method entailing third-order ($m = 3$) GPCE approximations was applied to solve this elementary RBDO problem. To assess the accuracy of the proposed method, a benchmark solutions, named MCS/FD, was obtained by crude MCS involving 1×10^6 samples for reliability analysis and the central finite-difference approximation for design sensitivity analysis. The approximate optimal solutions are denoted by $\tilde{\mathbf{d}}^* = (\tilde{d}_1^*, \tilde{d}_2^*)^\intercal$.

Table 3 summarizes the optimization results for the three aforementioned cases of the correlation coefficient and three different initial designs. Consider first the RBDO results when the initial design is $\mathbf{d}_0 = (5, 5)^\intercal$. As shown in the second and third columns from the left in Table 3, the respective RBDO solutions generated by the MPSS-GPCE (proposed) and MCS/FD (benchmark) methods are practically identical for all three correlation coefficients. According to both of these methods, there are two active constraints $c_2 \simeq 0$ and $c_3 \simeq 0$ and one inactive constraint $c_1 = -\Phi(-3) \simeq -1.35 \times 10^{-3}$. The reported solutions by PMA+ (Noh et al. 2009), included in the fourth column, are also accurate, although there is a palpable improvement in the results of the MPSS-GPCE method over those of PMA+. The PMA+ solution involved a copula, which was easy to guess when the input random variables are Gaussian. Nonetheless, these solutions obtained by all three methods are very close to each other, confirming the accuracy of the final optimal solution by the proposed method. Furthermore, for three correlation coefficients, the MPSS-GPCE method requires only 150–330 function evaluations, which are fractions of the hundred million function evaluations demanded by MCS/FD. Therefore, the proposed method is not only accurate but also economical.

The fifth and sixth columns in Table 3 enumerate the optimal design solutions obtained by the MPSS-GPCE and MCS/FD methods using the remaining two initial designs: $\mathbf{d}_0 = (1, 1)^\intercal$ and $\mathbf{d}_0 = (9, 4)^\intercal$. Whether starting from the former initial design ($\mathbf{d}_0 = (5, 5)^\intercal$) or the latter two initial designs ($\mathbf{d}_0 = (1, 1)^\intercal$, $\mathbf{d}_0 = (9, 4)^\intercal$), the proposed method yields nearly indistinguishable optimal solutions for each case of the correlation coefficient, thus affirming its

Table 3 Optimization results for the mathematical problem (Example 1)

	$\mathbf{d}_0 = (5,5)^\intercal$			$\mathbf{d}_0 = (1,1)^\intercal$	$\mathbf{d}_0 = (9,4)^\intercal$
	MPSS-GPCE[a]	MCS/FD[b]	PMA+[c]	MPSS-GPCE[a]	MPSS-GPCE[a]
Case 1: Correlation coefficient = 0.4					
$\tilde{d}_1^*$	5.6332	5.6375	5.622	5.6336	5.6329
$\tilde{d}_2^*$	3.4965	3.4960	3.516	3.4963	3.4965
$c_0(\tilde{\mathbf{d}}^*)$	−2.1367	−2.1415	−2.105	−2.1374	−2.1364
$c_1(\tilde{\mathbf{d}}^*)$[d]	-1.3499×10^{-3}	-1.3499×10^{-3}	-[e]	-1.3499×10^{-3}	-1.3499×10^{-3}
$c_2(\tilde{\mathbf{d}}^*)$[d]	1.0197×10^{-7}	1.0197×10^{-7}	-[e]	1.0197×10^{-7}	1.0197×10^{-7}
$c_3(\tilde{\mathbf{d}}^*)$[d]	-4.6898×10^{-5}	1.0197×10^{-7}	-[e]	-4.2898×10^{-5}	-4.8898×10^{-5}
Case 2: Correlation coefficient = −0.4					
$\tilde{d}_1^*$	6.1590	6.1575	6.145	6.1590	6.1590
$\tilde{d}_2^*$	3.2554	3.2556	3.271	3.2554	3.2554
$c_0(\tilde{\mathbf{d}}^*)$	−2.9036	−2.9019	−2.874	−2.9036	−2.9036
$c_1(\tilde{\mathbf{d}}^*)$[d]	-1.3499×10^{-3}	-1.3499×10^{-3}	-[e]	-1.3499×10^{-3}	-1.3499×10^{-3}
$c_2(\tilde{\mathbf{d}}^*)$[d]	-8.9803×10^{-7}	2.1020×10^{-6}	-[e]	1.0197×10^{-7}	-8.9803×10^{-7}
$c_3(\tilde{\mathbf{d}}^*)$[d]	2.9102×10^{-5}	1.1020×10^{-6}	-[e]	2.7102×10^{-5}	2.8102×10^{-5}
Case 3: Correlation coefficient = 0					
$\tilde{d}_1^*$	5.8616	5.8605	5.846	5.8616	5.8622
$\tilde{d}_2^*$	3.4125	3.4128	3.4330	3.4125	3.4124
$c_0(\tilde{\mathbf{d}}^*)$	−2.4492	−2.4477	−2.414	−2.4491	−2.4499
$c_1(\tilde{\mathbf{d}}^*)$[d]	-1.3499×10^{-3}	-1.3499×10^{-3}	-[e]	-1.3499×10^{-3}	-1.3499×10^{-3}
$c_2(\tilde{\mathbf{d}}^*)$[d]	1.0197×10^{-7}	1.0197×10^{-7}	-[e]	1.0197×10^{-7}	-8.9803×10^{-7}
$c_3(\tilde{\mathbf{d}}^*)$[d]	1.4102×10^{-5}	1.0197×10^{-7}	-[e]	1.4102×10^{-5}	2.2102×10^{-5}

[a]The MPCE-GPCE method employing third-order ($m = 3$) GPCE approximations was employed

[b]Crude MCS with 1×10^6 sample size was employed for reliability analysis and design sensitivity analysis based on the central finite-difference method

[c]The results of PMA+ are from Noh et al. (2009)

[d]The constraint values are calculated by crude MCS with 10^6 sample size

[e]The probabilistic constraint value at the optimal design is not provided by Noh et al. (2009)

robustness in solving this RBDO problem. No PMA+ solutions have been reported for these two initial designs.

In order to better understand the performance of the MPSS-GPCE method, Fig. 5a–c depict its iteration histories in the two-dimensional design space $\mathcal{D} = [0, 10] \times [0, 10] \subset \mathbb{R}^2$, obtained for all three correlation coefficients and all three initial designs. The design space was discretized by a 100×100 grid, producing a total of 10,000 grid points. At each grid point, the estimates of three probabilistic constraint functions c_l, $l = 1, 2, 3$, were obtained using crude MCS with a sample size of 2×10^6. In Fig. 5a or c, the first initial design $(5, 5)^\intercal$ lies in the infeasible domain for the correlation coefficient 0.4 or 0, respectively, whereas in Fig. 5b, the same initial design is located in the feasible domain for the correlation coefficient −0.4. In contrast, the last two initial designs $(1, 1)^\intercal$ and $(9, 4)^\intercal$ lie in the infeasible domains for all three correlation coefficients in Fig. 5a–c. Notwithstanding that the two initial designs $(1, 1)^\intercal$ and $(9, 4)^\intercal$ are situated further from the feasible domain than $(5, 5)^\intercal$, the proposed RBDO method adjusts the infeasible initial designs to feasible ones through the interpolation process, explained in Step 8 of Fig. 3, and then delivers almost identical optimum solutions to those from $(5, 5)^\intercal$ after solving a few subregion problems ($Q' = 4 - 9$). Therefore, these optimization results demonstrate how the proposed method can be effectively used to solve an RBDO problem, whether or not the initial design is feasible.

Furthermore, Fig. 5a–c illustrate that the optimal solutions rely on the correlation between input random variables X_1 and X_2. Indeed, the boundaries of feasible domains, formed by three probabilistic constraints $c_l(\mathbf{d}) = 0$, $l = 1, 2, 3$, are altered for different correlation coefficients, thus resulting in three different optimal designs, $(5.3, 3.5)^\intercal$, $(6.2, 3.3)^\intercal$, and $(5.9, 3.4)^\intercal$, respectively. Hence, such correlations, if they exist, among input random variables should be accounted for during design optimization under uncertainty.

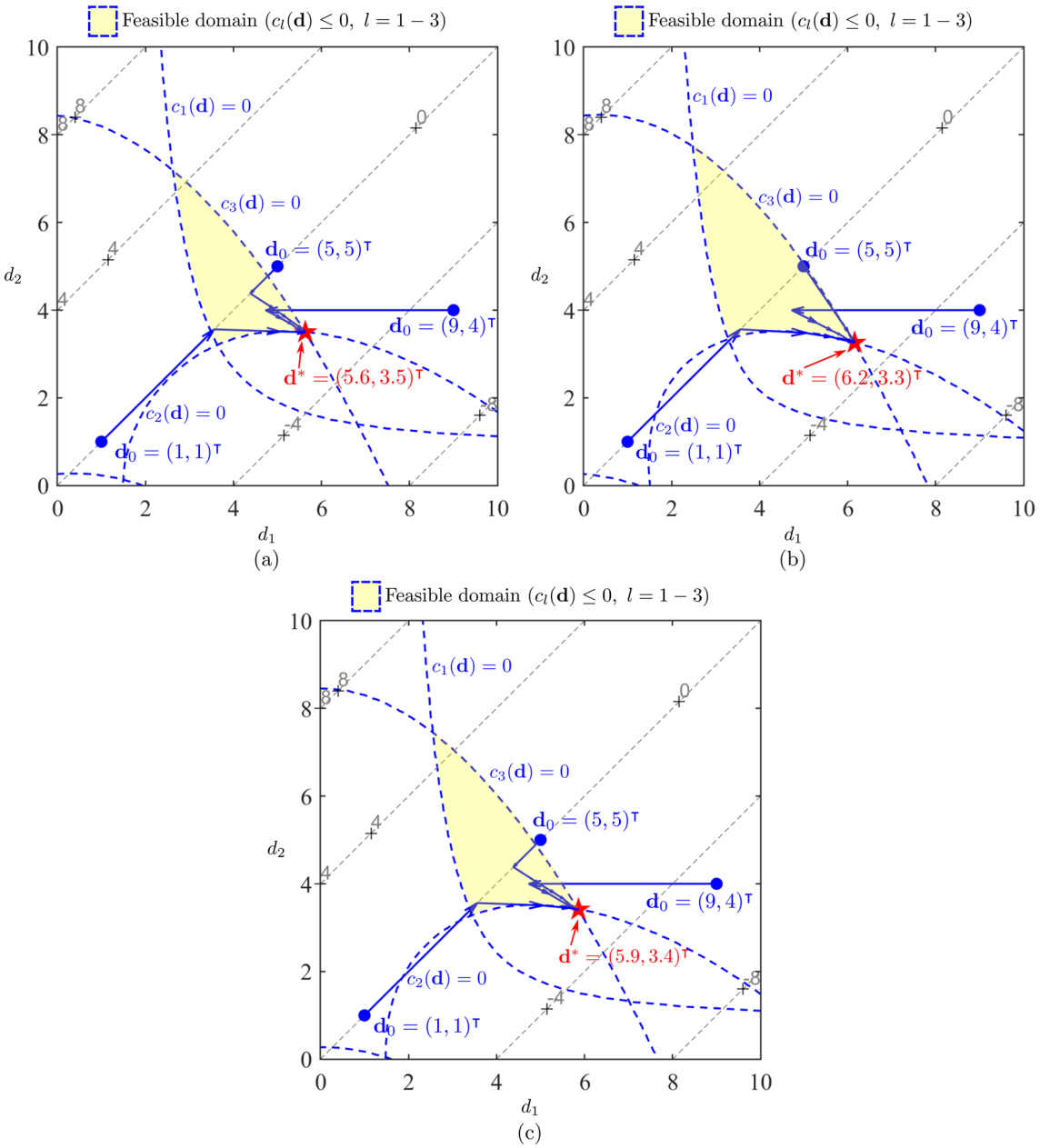

Fig. 5 Iteration histories (q') of the MPSS-GPCE method for three different initial designs in Example 1: **a** correlation coefficient = 0.4; **b** correlation coefficient = −0.4; and **c** correlation coefficient = 0. Here, the initial designs are $\mathbf{d}_0$ (blue dots), the optimal designs are $\mathbf{d}^*$ (red stars), and the boundaries of constraint functions are $c_l(\mathbf{d}) = 0$, $l = 1, 2, 3$ (blue dotted lines)

6.2 Example 2: Size design of an eccentric loaded column

The second example was created by recasting an eccentrically loaded column problem, formerly investigated in the context of deterministic optimization by Arora (2004). This example intends to prove the technical merit of the proposed method when confronted with highly nonlinear performance functions in solving RBDO problems. As shown in Fig. 6, there are four input random variables $\mathbf{X} = (X_1, X_2, X_3, X_4)^\intercal$, where X_1 and X_2 are means of the average radius (average of outer and inner radii) and the thickness, respectively, of a hollow circular tube of length X_4. The tubular column is subject to a deterministic load with eccentricity $0.01X_3X_1$ about its center axis. It is made of cast iron, which has Young's modulus $E = 210$ GPa. The design variables are $d_1 = \mathbb{E}_{\mathbf{d}}[X_1]$ and $d_2 = \mathbb{E}_{\mathbf{d}}[X_2]$, and X_1 and X_2 follow a bivariate lognormal distribution with the correlation coefficient 0.7982. The probability distributions of all input random variables are listed in Table 4.

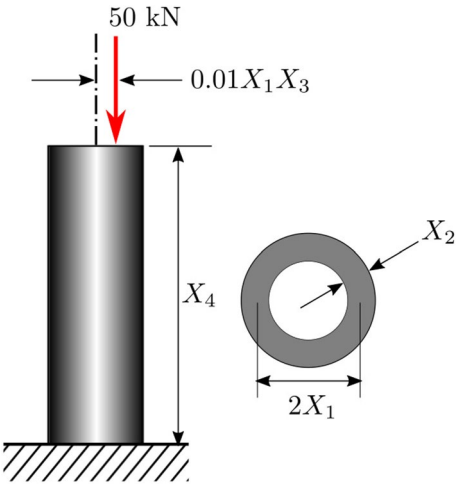

Fig. 6 Configuration of the vertical column with an eccentric load (Example 2)

Table 4 Statistical properties of random variables of the column with an eccentric load (Example 2)

Random variables	Mean	Standard deviation	Probability distribution
X_1, m[a]	d_1	$0.15d_1$	Lognormal
X_2, m[a]	d_2	$0.15d_2$	Lognormal
X_3	3	0.1	Weibull
X_4, m	5	0.05	Normal

[a] X_1 and X_2 are dependent with the correlation coefficient of 0.7982

The objective of this RBDO problem is to minimize the volume of the hollow circular tube, calculated when the random geometric variables assume their respective means. Three probabilistic constraints, described in (25), (26), and (27), limit the normal stress, buckling load, and deflection at or below the respective thresholds of the allowable stress $\sigma_a = 2.5 \times 10^8$ Pa and lateral deflection $\Delta = 0.25$ m. The deterministic constraint c_4 in (24) restricts the ratio of d_1/d_2, not to exceed the value of 50 for practical considerations. Mathematically, such an RBDO problem is devised to

$$\begin{aligned} &\min_{\mathbf{d}\in\mathcal{D}\subseteq\mathbb{R}^M} c_0(\mathbf{d}) := V(\mathbf{d}),\\ &\text{subject to } c_l(\mathbf{d}) := \mathbb{P}_{\mathbf{d}}[y_l(\mathbf{X}) < 0] - \Phi(-3) \le 0,\\ &l = 1, 2, 3,\\ &c_4(\mathbf{d}) := -1 + \frac{d_1}{50d_2} \le 0,\\ &0.01 \text{ m} \le d_1 \le 1 \text{ m},\\ &0.005 \text{ m} \le d_2 \le 0.2 \text{ m}, \end{aligned} \tag{24}$$

where

$$y_1(\mathbf{X}) = 1 - \frac{50\times10^3}{2\pi X_1X_2\sigma_a}\left[1 + \frac{2\times0.01X_3(X_1+0.5X_2)}{X_1} \times\sec\left(\frac{\sqrt{2}X_4}{X_1}\sqrt{\frac{50\times10^3}{E(2\pi X_1X_2)}}\right)\right], \tag{25}$$

$$y_2(\mathbf{X}) = 1 - \frac{200\times10^3X_4^2}{\pi^3EX_1^3X_2}, \tag{26}$$

$$y_3(\mathbf{X}) = 1 - \frac{0.01X_3X_1}{\Delta}\left[\sec\left(\sqrt{\frac{50\times10^3}{E\pi X_1^3X_2}}\right) - 1\right] \tag{27}$$

are three random performance functions of the normal stress, buckling load, and deflection, respectively. In (24), the total volume of the column at mean values of input is $V(\mathbf{d}) \approx 10\pi d_1d_2$. The initial design is $\mathbf{d}_0 = (1, 0.2)^\intercal$ m.

Table 5 presents detailed optimization results from the MPSS-GPCE method, obtained employing fourth- ($m = 4$), fifth- ($m = 5$), and sixth-order ($m = 6$) GPCE approximations. The corresponding results are listed in the second, third, and fourth columns, respectively, from the left. The optimal solutions by the proposed methods, regardless of m, are very close to each other, satisfying practically all constraint conditions. Although there is a slight constraint violation for the second probabilistic constraint ($c_2 > 0$), it is considered to be active due to its negligibly small value with respect to its target failure probability $\Phi(-3) \approx 1.35 \times 10^{-3}$.

To evaluate the accuracy of the RBDO solutions from the multi-point single-step method, two benchmark solutions were created. The first benchmark solution, named MCS/FD and presented in the fifth column, involves crude MCS for reliability analysis and finite-difference approximation for design sensitivity analysis. However, to overcome its high computational cost, the initial design was selected to be the sixth-order MPSS-GPCE solution (fourth column), thus minimizing the needed design iterations as much as possible. The second benchmark solution, referred to as MCS/SF and tabulated in the sixth column, entails crude MCS for reliability analysis but score functions for design sensitivity analysis. The initial design for the second benchmark solution is the same as the one used for the proposed RBDO solutions. The sample size of MCS in both benchmark solutions is 1×10^6. The comparisons between the benchmark solutions and those obtained by the proposed RBDO solutions are remarkably close, thereby affirming the accuracy of the final optimal designs by the multi-point single-step method. However, the proposed method reduces the computational cost dramatically, demanding only 5,460–16,38 function evaluations, which are fractions of the tens of millions of function evaluations required by the MCS-based benchmark solutions.

Table 5 Optimization results for the vertical column design problem (Example 2)

	MPSS-GPCE				
	$m = 4$[a]	$m = 5$[a]	$m = 6$[a]	MCS/FD[b]	MCS/SF[c]
$\tilde{d}_1^*$	0.0951	0.0937	0.0959	0.0959	0.0964
$\tilde{d}_2^*$	0.0050	0.0055	0.0050	0.0050	0.0050
$c_0(\tilde{\mathbf{d}}^*)$	0.0149	0.0161	0.0151	0.0151	0.0151
$c_1(\tilde{\mathbf{d}}^*)$[d]	-1.2179×10^{-3}	-1.2159×10^{-3}	-1.2249×10^{-3}	-1.2267×10^{-3}	-1.2149×10^{-3}
$c_2(\tilde{\mathbf{d}}^*)$[d]	3.7710×10^{-4}	-5.9898×10^{-5}	1.4010×10^{-4}	1.3630×10^{-4}	-8.9803×10^{-7}
$c_3(\tilde{\mathbf{d}}^*)$[d]	-1.3499×10^{-3}	-1.3499×10^{-3}	-1.3499×10^{-3}	-1.3499×10^{-3}	-1.3499×10^{-3}
$c_4(\tilde{\mathbf{d}}^*)$	-6.1968×10^{-1}	-6.5802×10^{-1}	-6.1624×10^{-1}	-6.1624×10^{-1}	-6.1428×10^{-1}
No. of y_l eval., $l = 1, 2, 3$	5, 460	10, 206	16, 380	2, 950, 000, 000	34, 000, 000
No. of y_4 evaluation	151	164	161	59	34

[a]The degree (m) of GPCE approximation

[b]Crude MCS with 10^6 sample size for reliability analysis and design sensitivity analysis based on the central finite-difference method; the initial design was set to the optimal solution of the sixth-order ($m = 6$) multi-point single-step GPCE method

[c]Crude MCS with 10^6 sample size for reliability analysis and design sensitivity analysis based on the score function method; the initial design was set to the original initial design $\mathbf{d}_0 = (1, 0.2)^\intercal$

[d]The constraint values were estimated by crude MCS with 10^6 sample size

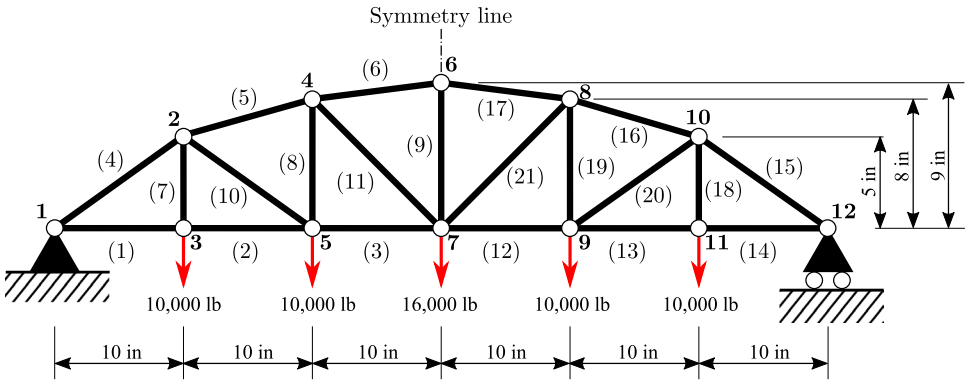

Fig. 7 Configuration of the six-bay, twenty-one-bar truss structure (Example 3)

6.3 Example 3: Optimal sizing design of a six-bay, twenty-one-bar truss

The third example demonstrates the ability of the proposed method in solving an RBDO problem involving system reliability constraints. Fig. 7 depicts a linear-elastic, six-bay, twenty-one-bar truss structure, originally studied by (Ren et al. 2016). It is simply supported at nodes 1 and 12 and is subject to four concentrated loads of 10,000 lb (44,482 N) at nodes 3, 5, 9, and 11, respectively, and a concentrated load of 16,000 lb (71,172 N) at node 7. The truss is made of an aluminum alloy with the Young's modulus $E = 10^7$ psi (68.94 GPa).

There are twenty-one ($N = 21$) random variables $\mathbf{X} = (X_1, \ldots, X_{21})^\intercal$ representing the cross-sectional areas of all twenty bars. Unlike the previous study (Ren et al. 2016), these random variables follow correlated lognormal distributions, which have means $\mathbb{E}_{\mathbf{d}}[X_i]$, $i = 1, \ldots, 21$; standard deviations $0.1\mathbb{E}_{\mathbf{d}}[X_i]$, $i = 1, \ldots, 21$; and correlation coefficients $\rho_{ij} = 0.5988$, $i, j = 1, \ldots, 21$, $i \neq j$. The means of $\mathbf{X}$ are all set as design variables, that is, $d_k := \mathbb{E}_{\mathbf{d}}[X_k]$, $k = 1, \ldots, 21$.

Determined from a linear-elastic FEA, the maximum vertical displacement $v_{\max}(\mathbf{X})$ and maximum axial stress $\sigma_{\max}(\mathbf{X})$ are limited by the permissible values of $d_{\text{allow}} = 0.266$ in (6.76 mm) and $\sigma_{\text{allow}} = 37,680$ psi (259.8 MPa), respectively. The nodes at which these maximum physical values occur can shift depending on the changes in the means of the cross-sectional areas during the optimization process. The system-level failure set is defined as $\Omega_F := \{\mathbf{x} : \{y_1(\mathbf{x}) < 0\} \cup \{y_2(\mathbf{x}) < 0\}\}$, where the performance functions

$$y_1(\mathbf{X}) = 1 - \frac{|v_{\max}(\mathbf{X})|}{d_{\text{allow}}}, \; y_2(\mathbf{X}) = 1 - \frac{|\sigma_{\max}(\mathbf{X})|}{\sigma_{\text{allow}}}.$$

For the RBDO problem, the objective is to minimize the volume of the truss, calculated at mean cross-sectional areas,

Table 6 Optimization results for the six-bay, 21-bar truss problem (Example 3)

	Case 1 (without the symmetry condition)		Case 2 (with the symmetry condition)	
	MPSS-GPCE[(a)]	MCS/SF[(b)]	MPSS-GPCE[(a)]	MCS/SF[(b)]
$\tilde{d}_1^*$	3.7922	3.9103	3.8497	3.9320
$\tilde{d}_2^*$	4.1494	4.2432	3.9691	3.8865
$\tilde{d}_3^*$	4.3534	4.3490	4.3705	4.4173
$\tilde{d}_4^*$	4.0770	4.2448	4.1482	4.2876
$\tilde{d}_5^*$	4.5972	4.5695	4.6146	4.6347
$\tilde{d}_6^*$	5.4279	5.5801	5.2380	5.2985
$\tilde{d}_7^*$	1.0000	1.0000	1.0000	1.0000
$\tilde{d}_8^*$	1.0000	1.0000	1.0000	1.0000
$\tilde{d}_9^*$	1.0000	1.0280	1.0000	1.0000
$\tilde{d}_{10}^*$	1.0000	1.0000	1.0000	1.0000
$\tilde{d}_{11}^*$	1.0023	1.0000	1.0000	1.0000
$\tilde{d}_{12}^*$	4.1815	4.1256	4.3705[(c)]	4.4173[(c)]
$\tilde{d}_{13}^*$	3.8101	3.9231	3.9691[(c)]	3.8865[(c)]
$\tilde{d}_{14}^*$	3.4667	3.6848	3.8497[(c)]	3.9320[(c)]
$\tilde{d}_{15}^*$	4.4683	4.4063	4.1482[(c)]	4.2876[(c)]
$\tilde{d}_{16}^*$	4.5358	4.4057	4.6146[(c)]	4.6347[(c)]
$\tilde{d}_{17}^*$	5.3795	5.2284	5.2380[(c)]	5.2985 [(c)]
$\tilde{d}_{18}^*$	1.0000	1.0000	1.0000[(c)]	1.0000[(c)]
$\tilde{d}_{19}^*$	1.0000	1.0000	1.0000[(c)]	1.0000[(c)]
$\tilde{d}_{20}^*$	1.0000	1.0000	1.0000[(c)]	1.0000[(c)]
$\tilde{d}_{21}^*$	1.0000	1.0000	1.0000[(c)]	1.0000[(c)]
$c_0(\tilde{\mathbf{d}}^*)$	620.04	624.64	621.15	626.84
$c_1(\tilde{\mathbf{d}}^*)$[(d)]	5.8277×10^{-4}	4.3530×10^{-7}	7.1544×10^{-4}	1.6102×10^{-5}
No. of FEA	14, 421	528, 000, 000	5, 382	477, 000, 000

[a]The MPSS-GPCE method of second-order ($m = 2$) GPCE approximations was employed

[b]Crude MCS with 3×10^6 sample size for reliability analysis and design sensitivity analysis based on the score function method

[c]The value is obtained from the symmetry condition

[d]The constraint value was estimated by crude MCS with 3×10^6 sample size

such that the system reliability constraint forcing $v_{\max}(\mathbf{X})$ and $\sigma_{\max}(\mathbf{X})$ at or below their respective thresholds defined earlier. That is, the RBDO problem is formulated to

$$\min_{\mathbf{d} \in \mathcal{D} \subseteq \mathbb{R}^M} c_0(\mathbf{d}) := V(\mathbf{d}),$$
$$\text{subject to } c_1(\mathbf{d}) := \mathbb{P}_{\mathbf{d}}[\{y_1(\mathbf{X}) < 0\} \cup \{y_2(\mathbf{X}) < 0\}] - \Phi(-3) \leq 0,$$
$$1 \text{ in}^2 \leq d_k \leq 30 \text{ in}^2, \; k = 1, \ldots, 21.$$

The chosen initial design is $\mathbf{d}_0 = (15, \ldots, 15)^\intercal \text{ in}^2$, whereas the approximate final optimal design is denoted by $\tilde{\mathbf{d}}^* = (\tilde{d}_1^*, \ldots, \tilde{d}_{21}^*)^\intercal$.

The second column from the left in Table 6 presents the optimization results obtained by the proposed MPSS-GPCE method employing second-order ($m = 2$) GPCE approximations of y_1 and y_2. To produce a reference solution, crude MCS entailing 3×10^6 samples for reliability analysis and design sensitivity analysis based on the score function method was employed. The reference solution, denoted by MCS/FD, has its results tabulated in the third column. The comparison of optimization results from these two methods indicates that the proposed RBDO solution is very close to the reference solution by MCS/FD; however, the former requires only 14,421 FEA in contrast to 528 million FEA mandated by the latter. Therefore, the multi-point single-step method developed is not only highly accurate but also computationally efficient. The optimal designs from both methods reveal constraint violations by negligibly small values. Thus, they can be viewed practically as active constraints.

Given the symmetry in the loading and truss configuration, it is conceivable that the RBDO problem can be

recast by reducing the number of input random variables from 21 to 11, as done in a past work (Ren et al. 2016). Henceforth, the reduced RBDO problem involving $\mathbf{X} = (X_1, \ldots, X_{11})^\intercal$ and invoking the symmetry in cross-sectional areas of truss members was solved using the two aforementioned methods. The statistical properties of this reduced input vector are the same as before, but there are no separate random variables associated with truss members 12 through 21. The corresponding optimization results by the multi-point single-step method and MCS/FD solution are listed in the fourth and fifth columns of Table 6, respectively. Again, the proposed method delivers an accurate and computationally efficient RBDO solution for this problem. Due to a reduced number of random variables, the multi-point single-step method requires only 5382 FEA, whereas 477 million FEA are necessary to generate the MCS/FD solution.

Finally, the optimization results obtained using the full truss geometry and symmetric truss geometry should not be expected to be identical. Although some design variables have the same optimal values, there are other optimal design variables that are dissimilar. This is because the two optimization problems in the context of RBDO are fundamentally different, possibly yielding distinct design solutions. Therefore, imposing such a symmetry condition may not be suitable when solving design problems in the presence of correlated or dependent input random variables.

6.4 Example 4: Shape optimization of a jet engine compressor blade root

This last example demonstrates the high performance of the proposed RBDO method in solving an industrial-scale shape design problem, encompassing a gas turbine jet engine in an aircraft, as shown in Fig. 8a. The jet engine includes a compressor section, as shown in Fig. 8a, for pressurizing incoming air mixed with fuels before it enters the combustion chamber and then gets ignited. For the compressor, individual blades are attached to a disk through joining parts, referred to as a blade root and a disk groove, depicted in Fig. 8a. When the blades are installed, the disk acts as an anchoring component for the turbine blades. As a result, the blades can transmit to the disk the energy they extract from the exhaust gases.

In general, such a blade root attachment permits blades to be easily replaced, thus saving maintenance costs. The blade roots need to be designed to maintain fatigue durability under harsh environments, such as high temperature, high pressure, or high centrifugal loading, sustaining its performance during the expected service lifetime. Otherwise, it may cause catastrophic failure. However, uncertainties in manufacturing variables or material properties exist inherently, resulting in the randomness of fatigue life. As a conservative design approach, a large safety factor is applied to ensure its satisfactory long-term performance, but it may cause an unnecessary blade weight increment and, hence, fuel efficiency loss. Thus, reliability analysis of fatigue life should be accounted for when designing a lightweight blade/disk attachment geometry. Such optimal design can be achieved through the RBDO process developed in this work.

In Fig. 8b, the left figure depicts a computer-aided design (CAD) model of a sector of the blade/disk assembly, and the right two figures present its blade root including a total of 14 random manufacturing variables $\mathbf{X} = (X_1, \ldots, X_{14})^\intercal$. Of these random variables, (1) X_1 through X_{11} describe the outer profile of the blade root cross-section; (2) X_{12} and X_{13} are the width and the height, respectively, of four holes in the blade root, created to reduce the volume as much as possible; and (3) X_{14} is the depth of the blade root. The 14-dimensional ($N = 14$) input random vector $\mathbf{X}$ follows a multivariate log-normal distribution with means $\mathbb{E}_{\mathbf{d}}[X_i]$, $i = 1, \ldots, 14$; standard deviations $0.05\mathbb{E}_{\mathbf{d}}[X_i]$, $i = 1, \ldots, 14$; and correlation coefficients $\rho_{ij} = 0.4997$, $i,j = 1, \ldots, 14$. There are 14 design variables, that is, $d_k = \mathbb{E}_{\mathbf{d}}[X_k]$, $k = 1, \ldots, 14$. The respective disk groove always has the same outer shape as the blade root to be properly fitted together during design optimization. The jet engine compressor blade and disk are made of Titanium Alloy Ti-6Al-4V with the following deterministic material properties: mass density $\rho = 4430$ kg/m^3, elastic modulus $E = 115$ GPa, and Poisson's ratio $\nu = 0.33$. The deterministic fatigue parameters are as follows: fatigue strength coefficient $\sigma_f' = 2030$ MPa, fatigue strength exponent $b = -0.104$, fatigue ductility coefficient $\epsilon_f' = 0.841$, and fatigue ductility exponent $c = -0.69$.

The probabilistic performances of the blade and the disk were determined by fatigue durability analysis under the variable rotational speed of the engine compressor due to different flight conditions for takeoff, cruise, and land. It is assumed here that the compressor blade/disk assembly experiences constant-amplitude cyclic centrifugal forces determined by the maximum and minimum rotational speeds of 2100 rad/s and 0 rad/s, respectively. The fatigue durability analysis involved (1) calculating the maximum principal strain and the mean stress at a critical point; and (2) calculating the fatigue crack initiation life at that point from the well-known Coffin–Manson–Morrow equation (Stephens et al. 2000). The critical point is the location where the von-Mises stress is the largest, identified from FEA. As shown in Fig. 9a, the boundary condition involves fixing the bottom of the disk sector in all three directions and three axes of rotations, describing its geometric condition to be welded to the shaft. The junctions between surfaces of the blade root and the disk groove are enforced by tied contact constraints. The disk FEA model has rotational symmetry of the order 30 ($30 \times 12° = 360°$) on its left and right side borders, as

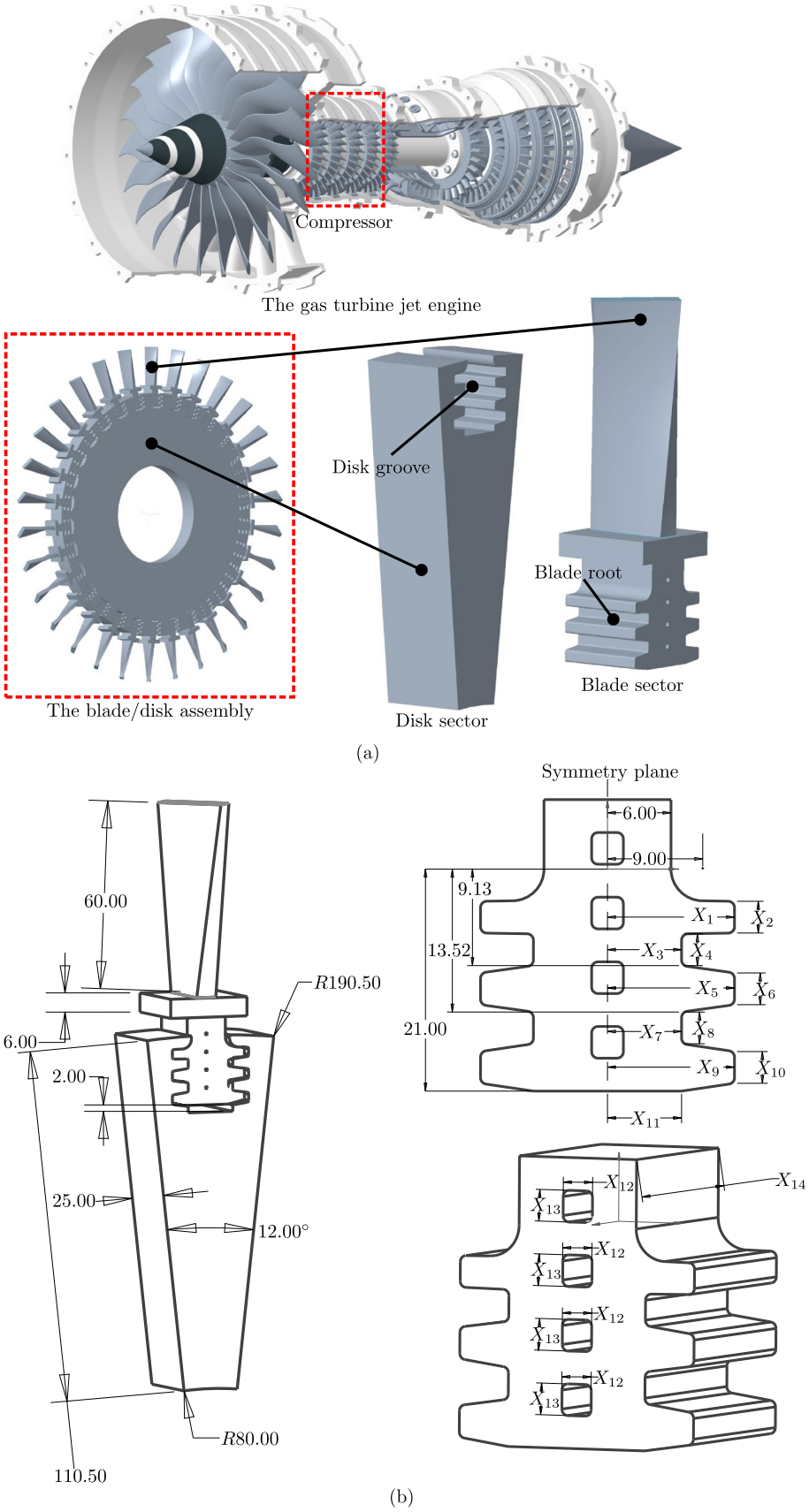

Fig. 8 The gas turbine jet engine (Example 4): **a** a photo of the blade/disk assembly; **b** a CAD model of a sector of the blade/disk assembly (left) and blade roots (right) (unit: mm)

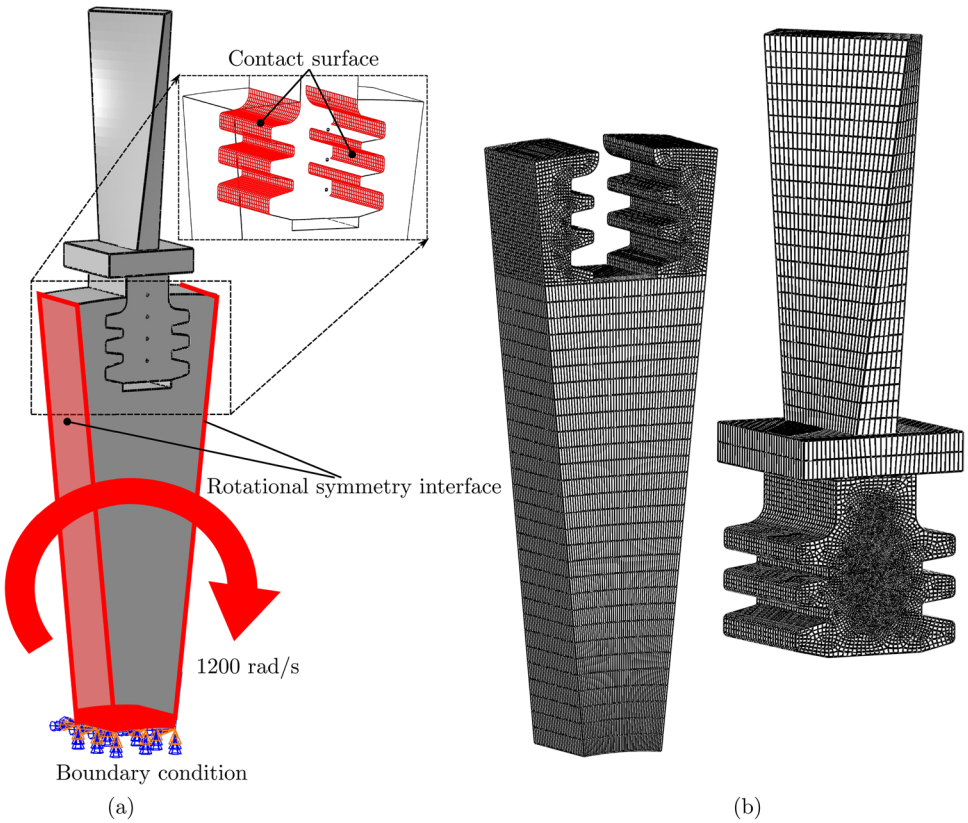

Fig. 9 An FEM of the compressor blade/disk assembly (Example 4): **a** boundary conditions and a centrifugal loading condition (the maximum rotational speed: 1200 rad/s); **b** hexahedral mesh comprising 203,026 elements

shown in 9a, and the whole body of the blade/disk assembly is presented in Fig. 8a.

For the RBDO problem, the objective is to minimize the volume of the blade root by changing the geometry such that the fatigue crack initiation lives $N_1(\mathbf{X})$ and $N_2(\mathbf{X})$ for the blade and the disk, respectively, under the cyclic loading conditions at the critical point exceed the design threshold of a half-million cycles with $(1-\Phi(-3))\times 100 = 99.865\%$ probability. Mathematically, the RBDO problem requires one to

$$\min_{\mathbf{d}\in\mathcal{D}} c_0(\mathbf{d}) := \frac{\mathbb{E}_{\mathbf{d}}[y_0(\mathbf{X})]}{\mathbb{E}_{\mathbf{d}_0}[y_0(\mathbf{X})]},$$

$$\begin{aligned}
&\text{subject to } c_1(\mathbf{d}) := \mathbb{P}_{\mathbf{d}}[y_1(\mathbf{X})<0]-\Phi(-3)\le 0,\\
&c_2(\mathbf{d}) := \mathbb{P}_{\mathbf{d}}[y_2(\mathbf{X})<0]-\Phi(-3)\le 0,\\
&10\text{ mm}\le d_1\le 12\text{ mm},\ 1\text{ mm}\le d_2\le 3\text{ mm},\\
&4\text{ mm}\le d_3\le 7\text{ mm},\ 1\text{ mm}\le d_4\le 3\text{ mm},\\
&9\text{ mm}\le d_5\le 12\text{ mm},\ 1\text{ mm}\le d_6\le 3\text{ mm},\\
&4\text{ mm}\le d_7\le 7\text{ mm},\ 1\text{ mm}\le d_8\le 3\text{ mm},\\
&8\text{ mm}\le d_9\le 12\text{ mm},\ 1\text{ mm}\le d_{10}\le 3\text{ mm},\\
&1\text{ mm}\le d_{11}\le 7\text{ mm},\ 0.5\text{ mm}\le d_{12}\le 4\text{ mm},\\
&0.5\text{ mm}\le d_{13}\le 4\text{ mm},\ 10\text{ mm}\le d_{14}\le 20\text{ mm},
\end{aligned}$$

where

$$y_0(\mathbf{X}) = \int_{\mathcal{D}'(\mathbf{X})} d\mathcal{D}'$$

is the random volume of the blade root, and

$$y_1(\mathbf{X}) = \log_{10}\left[\frac{N_1(\mathbf{X})}{5\times 10^5}\right]$$

and

$$y_2(\mathbf{X}) = \log_{10}\left[\frac{N_2(\mathbf{X})}{5\times 10^5}\right]$$

are stochastic performance functions given by log-scale normalized fatigue crack initiation lives for the blade root and the groove potion of the disk, respectively. The initial design $\mathbf{d}_0 = (d_{1,0},\ldots,d_{14,0})^\intercal$ mm is listed in Table 7. Figure 9b presents an FEA mesh for the initial design of a sector of the blade/disk assembly, which comprises 203,026 hexahedral elements. The approximate optimal solution is denoted by $\tilde{\mathbf{d}}^* = (\tilde{d}_1^*,\ldots,\tilde{d}_{14}^*)^\intercal$.

The MPSS-GPCE method, employing first-order ($m=1$) GPCE approximations for reliability analyses of $y_1(\mathbf{X})$ and $y_2(\mathbf{X})$, was applied in solving this RBDO problem. The selection of the low-order GPCE approximation is motivated by local design spaces where a high-order GPCE may not be needed, thereby reducing the

Table 7 Initial and optimal values of design variables for the jet engine compressor blade root (Example 4)

k	$d_{k,0}$ mm	$\tilde{d}_k^*$ mm
1	12	10.8318
2	3	1.9780
3	7	4.8823
4	2	3.0000
5	12	9.8823
6	3	1.8318
7	7	4.8823
8	2	2.8683
9	12	8.0000
10	3	1.8697
11	7	1.2515
12	0.5	3.9125
13	0.5	1.9360
14	20	10.0000

computational demand of the MPSS-GPCE method as much as possible.

The optimal design solutions are presented in the third column from the left in Table 7. At optimum, the design variables d_4^* and d_{14}^* reached their lower limits, but the rest of the design variables converged to values between their respective lower and upper limits, satisfying probabilistic constraints ($c_1 \simeq -0.0010$, $c_2 \simeq -0.0013$). The mean optimal volume of the blade root is 3409.0 mm^3, achieving a 65% reduction from the initial volume of 9707.7 mm^3. To complete the design process, the requisite number of FEA runs is 1, 425.

Figures 10a–d present the contour plots of the logarithm of the fatigue crack initiation life at the mean shapes of the blade root for several design iterations, including the initial design and the optimal design. The RBDO process started with a conservative initial design, such that the minimum fatigue crack initiation lives of 1.96×10^{14} cycles and 4.74×10^{14} cycles for the blade and the disk, respectively, are much larger than the target fatigue crack initiation life of a half-million cycles. Through the proposed method with tolerances and subregion size parameters appropriately selected, a total of 219 iterations (q) led to a final optimal design. Indeed, at optimum, there is a considerable reduction in the overall volume of the blade root, satisfying the target fatigue crack initiation life, as presented in Fig. 10d.

Figure 11 presents iterative histories (q) of the objective function value c_0 and normalized design variables $d_k/d_{k,0}$, k = 1–14, attained by the proposed method. In Fig. 11a, the objective function value decreases from 1 at the initial design to about 0.35 at the optimal design, resulting in an almost 65% reduction. However, the objective function converges non-monotonically with respect to design iteration (q) characterized by three distinct situations, as marked by A, B, and C in Fig. 11a. At mark A, the objective function decreases steeply with the single-step process for the first ($q' = 1$) subregion problem. At mark B, the rate of decrease becomes relatively slower, since the single-step process almost reaches convergence for the same subregion problem. After the convergence, the local optimal design is evaluated to determine whether or not it satisfies probabilistic constraints by new GPCE approximations recalculated by a new output data. If the constraints are fulfilled, then the optimal design is set to the initial design for the next subregion problem. Otherwise, the infeasible design is interpolated with the former feasible design to find a new feasible one, resulting in the fluctuation identified at mark C. The constraint violations at the optimal design by the single-step process are due to employing the relatively lower-order ($m = 1$) GPCE approximations with respect to the original performance functions. However, the multi-point approximation handles such error by restoring the infeasible design to a feasible one while continuously approaching the final optimal design and narrowing the next subregion size for a better convergence. Figures 11b and c show that all fourteen design variables have undergone moderate to substantial changes over iterations from their initial values, leading to the significant loss of the blade root volume while increasing its hole sizes. Note that the fatigue crack initiation lives for the blade root and disk groove were maintained above the target value of half-million cycles at the desired level of probability. Consequently, the minimum weight and target reliability of the blade root were both achieved, a distinctive advantage of RBDO over traditional deterministic design optimization. This culminating example confirms that the proposed RBDO method is capable of solving industrial-scale engineering design problems using only a few thousand FEA.

7 Discussion

This work should be distinguished from the earlier studies on UQ and design optimization conducted by the authors. Firstly, the underlying GPCE approximation was introduced by Lee and Rahman (2020) to tackle UQ problems for dependent random variables, but it does not provide a means to compute stochastic design sensitivities or design optimization. Secondly, the recently published paper by Lee and Rahman (2021) contains design sensitivity analysis, but it is limited to design optimization for robustness, not reliability. Thirdly, Ren et al. (2016) addressed RBDO problems, including formulating design sensitivity analysis and design optimization algorithms, but their work was restricted to independent random variables only. In contrast, the current study is new in the sense that a more general class of RBDO problems, tackling dependent input random variables head-on, is highlighted.

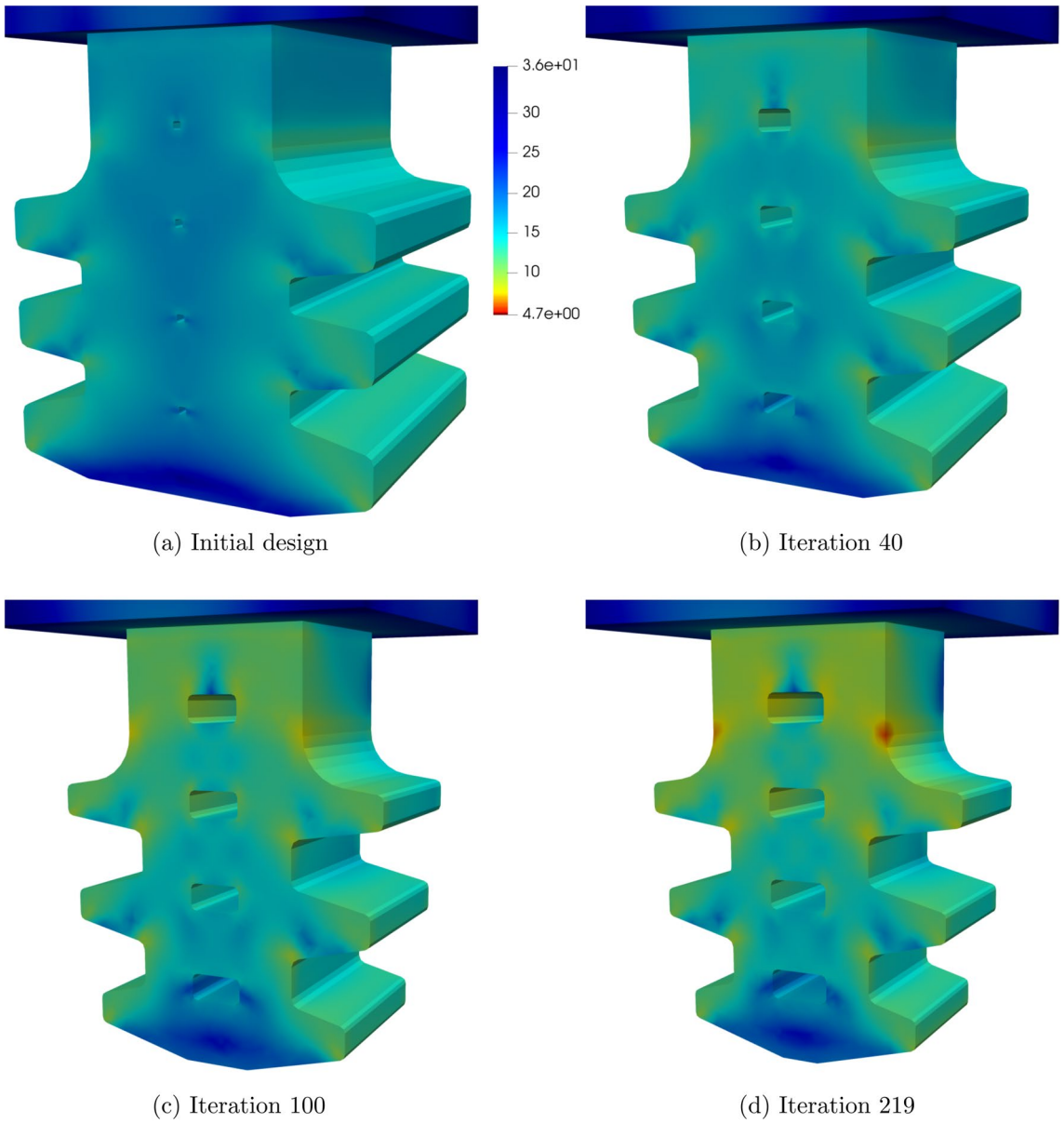

Fig. 10 Contours of logarithmic fatigue crack initiation life at the statistical mean shapes of the jet engine compressor blade root by the multi-point single-step design process employing 1st-order ($m = 1$) GPCE approximations (Example 4): **a** initial design; **b** iteration 40; **c** iteration 100; **d** iteration 219 (optimum)

The RBDO method developed here can be combined with RDO methods from the past (Lee and Rahman 2021) when the objective and/or constraint functions contain statistical moments of responses. Indeed, in Example 4, this was demonstrated by including the mean value of random geometric properties as the objective function. This may lead to a reliability-based robust design optimization framework for design under uncertainty.

For high-dimensional FEA-based RBDO problems, say, those involving 20 random or design variables, the GPCE approximation will require an astronomically large number of basis functions or coefficients, succumbing to the curse of dimensionality. Thus, developments of alternative RBDO methods capable of exploiting low effective dimensions of high-dimensional functions, such as those touted by the generalized polynomial dimensional decomposition (GPDD) (Rahman 2019), are desirable. In addition, variance-based importance measures or global sensitivity analysis (das Neves Carneiro and António 2020; das Neves Carneiro and Antonio 2021) may be employed to mitigate the curse of dimensionality by reducing essentially the size of an RBDO problem. In contrast, GPDD preserves all input

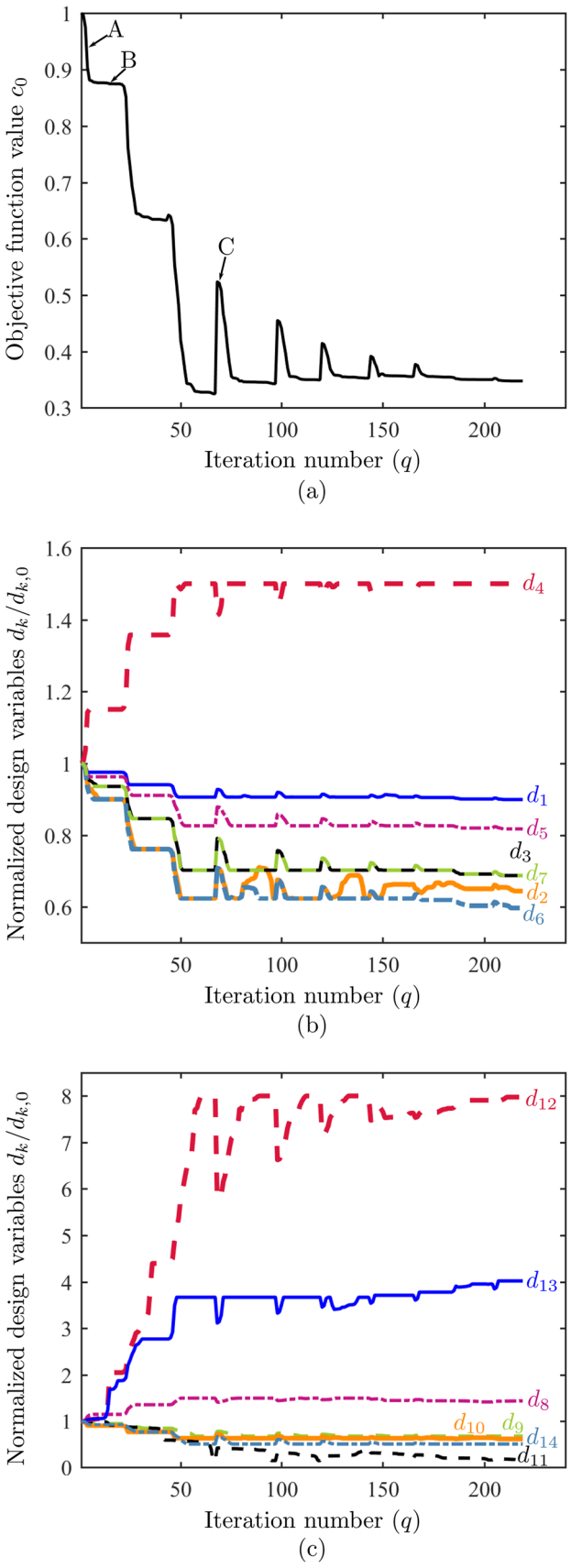

Fig. 11 RBDO iteration histories (q) for the compressor blade root design (Example 4): **a** objective function value c_0; **b** normalized design variables $d_k/d_{0,k}$ from $k = 1$ to $k = 7$; **c** normalized design variables $d_k/d_{0,k}$ from $k = 8$ to $k = 14$

random variables, while effectively reducing the number of basis functions in terms of interaction degrees between input random variables. Therefore, GPDD holds promise in tackling the curse of dimensionality for truly high-dimensional RBDO problems.

8 Conclusion

A new computational method, referred to as the multi-point single-step GPCE method or simply the MPSS-GPCE method, was devised for RBDO of complex mechanical systems in the presence of input random variables with arbitrary, dependent probability distributions. The method consists of three major components: (1) a GPCE for reliability analysis subject to dependent input random variables; (2) a novel fusion of the GPCE approximation and score functions for estimating the sensitivities of the failure probability with respect to design variables; and (3) standard gradient-based optimization algorithms, resulting in a multi-point single-step design process. When combined with score functions, the MPSS-GPCE method engenders analytical formulae for calculating the design sensitivities. More crucially, the failure probability and its design sensitivities are determined simultaneously from a single stochastic analysis or simulation, rendering the resultant MPSS-GPCE method computationally viable for generating optimal solutions.

Numerical results obtained from design optimization of mathematical functions and simple mechanical systems indicate adequate robustness of the MPSS-GPCE method, which provides not only highly accurate but also computationally efficient design solutions. Because of the local approach in the proposed RBDO method, a low-order GPCE approximation can be used for solving practical engineering problems, as demonstrated by shape design optimization of an industrial-scale jet engine compressor blade root.

Appendix 1: Statistical first-moment

Consider the mth-order GPCE approximation $h_m(\mathbf{Z};\mathbf{r})$ of $h(\mathbf{Z};\mathbf{r})$, presented in (12). Applying the expectation operator on $h_m(\mathbf{Z};\mathbf{r})$ and recognizing (7), its mean

$$\mathbb{E}_{\mathbf{g}}[h_m(\mathbf{Z};\mathbf{r})] = C_1(\mathbf{r}) = \mathbb{E}_{\mathbf{g}}[h(\mathbf{Z};\mathbf{r})] \tag{28}$$

coincides with the exact mean of $h(\mathbf{Z};\mathbf{r})$ for any $m \in \mathbb{N}_0$.

Appendix 2: Sensitivities of the first-moment

For $k = 1, \ldots, M$, consider the kth first-order score function $s_k(\mathbf{Z};\mathbf{g})$ in (17). Then, applying the full GPCE to $s_k(\mathbf{Z};\mathbf{g})$ leads to

$$s_k(\mathbf{Z};\mathbf{g}) = \sum_{i=2}^{\infty} D_{k,i}(\mathbf{g})\Psi_i(\mathbf{Z};\mathbf{g}),$$

with its GPCE coefficients

$$D_{k,i}(\mathbf{g}) = \int_{\mathbb{R}^N} s_k(\mathbf{z};\mathbf{g})\Psi_i(\mathbf{z};\mathbf{g}) f_{\mathbf{Z}}(\mathbf{z};\mathbf{g})d\mathbf{z}, \ i = 2, 3, \ldots, \infty.$$

Similarly, as shown in (16), by interchanging differential and integral operators and by replacing $h(\mathbf{Z};\mathbf{r})$ and $s_k(\mathbf{Z};\mathbf{g})$ with their mth-order and m'th-order GPCE approximations, respectively, for $m, m' \in \mathbb{N}_0$, the sensitivity of the first-moment with respect to d_k is formulated as follows:

$$\frac{\partial \mathbb{E}_{\mathbf{g}}[h_m(\mathbf{Z};\mathbf{r})]}{\partial d_k} = \frac{\partial g_k}{\partial d_k} \sum_{i=2}^{L_{\min}} C_i(\mathbf{r}) D_{k,i}(\mathbf{g}), \tag{29}$$

where $L_{\min} := \min(L_{N,m}, L_{N,m'})$. The approximate sensitivity in (29) converges to $\partial \mathbb{E}_{\mathbf{g}}[h(\mathbf{Z};\mathbf{r})] \,/\, \partial d_k$ when $m \to \infty$ and $m' \to \infty$.

Acknowledgements The authors acknowledge the financial support from the US National Science Foundation under Grant No. CMMI-1933114.

Declarations

Conflict of interest The authors declare that they have no conflict of interest.

Replication of results The results for Examples 1–4 provided in this paper were generated by MATLAB codes developed by the authors. In Example 4, the CAD model of the blade/disk assembly was created by CREO parametric. Then, the FE model was built and solved by ABAQUS/CAE. Finally, the fatigue crack initiation life was analyzed using an in-house MATLAB code. The CAD and FEA processes were fully integrated with the proposed RBDO algorithm for design automation by using MACRO functions and batch files in the MATLAB platform. The interested reader is encouraged to contact the corresponding author for further implementation details by e-mail.

References

ABAQUS (2019) version 2019. Dassault Systèmes Simulia Corp
Agarwal H, Renaud JE (2006) New decoupled framework for reliability-based design optimization. AIAA J 44(7):1524–1531
Arora JS (2004) Introduction to optimum design. McGraw-Hill, New York
Browder A (1996) Mathematical analysis: an introduction. Undergraduate texts in mathematics. Springer, Berlin
Chiralaksanakul A, Mahadevan S (2004) First-order approximation methods in reliability-based design optimization. J Mech Des 127(5):851–857
CREO (2016) version 4.0. PTC
das Neves Carneiro G, António CC (2020) Sobol' indices as dimension reduction technique in evolutionary-based reliability assessment. Eng Comput 37(1):368–398
das Neves Carneiro G, Antonio CC (2021) Dimensional reduction applied to the reliability-based robust design optimization of composite structures. Compos Struct 255:112937
Du X, Chen W (2004) Sequential optimization and reliability assessment method for efficient probabilistic design. J Mech Des 126(2):225–233
Fernandes AD, Atchley WR (2006) Gaussian quadrature formulae for arbitrary positive measures. Evol Bioinform. https://doi.org/10.1177/117693430600200010
Gautschi W (2004) Structural and multidisciplinary optimization. Numerical mathematics and scientific computation. Oxford University Press, Oxford
Gu X, Lu J, Wang H (2015) Reliability-based design optimization for vehicle occupant protection system based on ensemble of metamodels. Struct Multidiscip Optim 51(2):533–546
Hadigol M, Doostan A (2018) Least squares polynomial chaos expansion: a review of sampling strategies. Comput Methods Appl Mech Eng 332:382–407
Hassan R, Crossley W (2008) Spacecraft reliability-based design optimization under uncertainty including discrete variables. J Spacecraft Rockets 45(2):394–405
Kang B, Choi K, Kim DH (2017) An efficient serial-loop strategy for reliability-based robust optimization of electromagnetic design problems. IEEE Trans Magn 54(3):1–4
Kuschel N, Rackwitz R (1997) Two basic problems in reliability-based structural optimization. Math Methods Oper Res 46(3):309–333
Lee D, Rahman S (2020) Practical uncertainty quantification analysis involving statistically dependent random variables. Appl Math Model 84:324–356
Lee D, Rahman S (2021) Robust design optimization under dependent random variables by a generalized polynomial chaos expansion. Struct Multidiscip Optim 63(5):2425–2457
Lee I, Choi K, Du L, Gorsich D (2008) Dimension reduction method for reliability-based robust design optimization. Comput Struct 86(13–14):1550–1562
Lee I, Choi KK, Noh Y, Zhao L, Gorsich D (2011) Sampling-based stochastic sensitivity analysis using score functions for rbdo problems with correlated random variables. J Mech Des 10(1115/1):4003186
Lehkỳ D, Slowik O, Novák D (2018) Reliability-based design: artificial neural networks and double-loop reliability-based optimization approaches. Adv Eng Softw 117:123–135
Li L, Wan H, Gao W, Tong F, Li H (2019) Reliability based multidisciplinary design optimization of cooling turbine blade considering uncertainty data statistics. Struct Multidiscip Optim 59(2):659–673
Liang J, Mourelatos ZP, Nikolaidis E (2007) A single-loop approach for system reliability-based design optimization. J Mech Des 129(12):1215–1224
Luthen N, Marelli S, Sudret B (2021) Sparse polynomial chaos expansions: literature survey and benchmark. SIAM/ASA J Uncertain Quant 9(2):593–649
MATLAB (2019) version 9.7.0 (R2019b). The MathWorks Inc., Natick, Massachusetts
Nannapaneni S, Mahadevan S (2020) Probability-space surrogate modeling for fast multidisciplinary optimization under uncertainty. Reliab Eng Syst Saf 198:106896

Noh Y, Choi K, Du L (2009) Reliability-based design optimization of problems with correlated input variables using a Gaussian Copula. Struct Multidiscip Optim 38(1):1–16

Rahman S (2009) Extended polynomial dimensional decomposition for arbitrary probability distributions. J Eng Mech ASCE 135(12):1439–1451

Rahman S (2009) Stochastic sensitivity analysis by dimensional decomposition and score functions. Probab Eng Mech 24(3):278–287

Rahman S (2018) A polynomial chaos expansion in dependent random variables. J Math Anal Appl 464(1):749–775

Rahman S (2019) Uncertainty quantification under dependent random variables by a generalized polynomial dimensional decomposition. Comput Methods Appl Mech Eng 344:910–937

Rahman S, Wei D (2008) Design sensitivity and reliability-based structural optimization by univariate decomposition. Struct Multidiscip Optim 35(3):245–261

Ren X, Yadav V, Rahman S (2016) Reliability-based design optimization by adaptive-sparse polynomial dimensional decomposition. Struct Multidiscip Optim 53(3):425–452

Rosenblatt M (1952) Remarks on a multivariate transformation. Ann Math Stat 23:470–472

Rubinstein R, Shapiro A (1993) Discrete event systems: sensitivity analysis and stochastic optimization by the score function method. Wiley series in probability and mathematical statistics. Wiley, New York

Siavashi S, Eamon CD (2019) Development of traffic live-load models for bridge superstructure rating with rbdo and best selection approach. J Bridge Eng. https://doi.org/10.1061/(ASCE)BE.1943-5592.0001457

Stephens R, Fatemi A, Stephens RR, Fuchs H (2000) Metal fatigue in engineering. Wiley-Interscience, New York

Stieltjes TJ (1884) Quelques recherches sur la théorie des quadratures dites mécaniques. Ann Sci l'Écol Norm Supér 1:409–426

Suryawanshi A, Ghosh D (2016) Reliability based optimization in aeroelastic stability problems using polynomial chaos based metamodels. Struct Multidiscip Optim 53(5):1069–1080

Toropov V, Filatov A, Polynkin A (1993) Multiparameter structural optimization using FEM and multipoint explicit approximations. Struct Multidiscip Optim 6(1):7–14

Tu J, Choi KK, Park YH (1999) A new study on reliability-based design optimization. J Mech Des 121(4):557–564

Wiener N (1938) The homogeneous chaos. Am J Math 60(4):897–936

Xiu D, Karniadakis GE (2002) The Wiener–Askey polynomial chaos for stochastic differential equations. SIAM J Sci Comput 24:619–644

Yang IT, Hsieh YH (2013) Reliability-based design optimization with cooperation between support vector machine and particle swarm optimization. Eng Comput 29(2):151–163

Youn BD, Choi KK (2004) A new response surface methodology for reliability-based design optimization. Comput Struct 82(2–3):241–256

Youn BD, Choi K, Yang RJ, Gu L (2004) Reliability-based design optimization for crashworthiness of vehicle side impact. Struct Multidiscip Optim 26(3):272–283

Zhao L, Choi K, Lee I (2011) Metamodeling method using dynamic kriging for design optimization. AIAA J 49(9):2034–2046